

A NOVEL FORMULATION OF THE ADJOINT METHOD IN THE OPTIMAL DESIGN OF QUANTUM ELECTRONIC DEVICES*

A. F. J. LEVI[†] AND I. G. ROSEN[‡]

Abstract. The adjoint method is used to efficiently and accurately compute gradients with respect to the design parameters in the identification of optimal designs of electronic devices whose physical behavior is determined by solutions of the Schrödinger equation. In this study, the optimal design problem is formulated as the minimization of a least-squares performance metric. Key to our approach is the use of finite dimensional approximation based on the propagation matrix method and the reformulation of the underlying boundary value problem for an approximating time-independent Schrödinger equation as a terminal value problem. In this way the efficient computation of highly accurate gradients (i.e., with zero truncation error) required for optimization becomes amenable to the use of the adjoint method as it is typically applied in the context of evolution equations. The numerical stability of the method and the convergence of the approximating solutions to the state equations and their gradients with respect to the design parameters as well as the convergence of the solutions to the optimal design problems themselves are all rigorously established.

Key words. optimal design, nanoscale electronic device, Schrödinger equation, adjoint method

AMS subject classifications. 35J10, 65K10, 81V10

DOI. 10.1137/070708330

1. Introduction. Nonconvex optimal design can be used to discover nonintuitive configurations of atoms, molecules, and nanoparticles with a desired functionality determined by quantum mechanics [1]. A significant challenge in adoption of this methodology is the creation of computationally efficient design tools. With this in mind, we develop an efficient and accurate scheme for the determination of locally optimal designs for a prototype electronic device. More specifically we consider the optimal design of an electronic semiconductor device whose conduction band potential profile $V(x)$ can be fabricated with great accuracy in the crystal growth direction x . The design parameters are the values of the potential at each atomic layer, and the design criterion is a desired functional relationship between an applied voltage bias V_{bias} and electron transmission T . In the case of a resistor, by virtue of Ohm's law, this functional relationship is linear. Here, on the other hand, we are interested in devices that yield much more general functional relationships.

The determination of an optimal design will involve the solution of a constrained minimization or maximization problem in which the constraints involve solutions to boundary value problems for dynamical systems. Moreover, the design parameters will appear as coefficients, inputs, gains, etc. in the underlying differential equations. Our approach will use a form of the adjoint method to efficiently and accurately compute gradients with respect to these design parameters that are required when the resulting optimization problems are (necessarily) numerically solved. Key to our

*Received by the editors November 15, 2007; accepted for publication (in revised form) October 20, 2009; published electronically January 15, 2010. This research was supported in part by the Defense Advanced Research Projects Agency (DARPA) under contract N00014-05-10317 and in part by the Air Force Office of Scientific Research (AFOSR) under contract FA9550-07-1-048.

<http://www.siam.org/journals/sicon/48-5/70833.html>

[†]Department of Electrical Engineering, University of Southern California, 3620 S. Vermont Avenue, KAP 132, Los Angeles, CA 90089-2533 (alevi@usc.edu).

[‡]Department of Mathematics, University of Southern California, 3620 S. Vermont Avenue, KAP 104, Los Angeles, CA 90089-2532 (grosen@math.usc.edu).

approach is the use of finite dimensional approximation based on the propagation matrix method and the reformulation of the underlying boundary value problem for an approximating time-independent equation as a terminal value problem. In this way the efficient computation of highly accurate gradients required for optimization becomes amenable to the use of the adjoint method as it is typically applied in the context of evolution equations. We are able to rigorously establish the numerical stability of the method and the convergence of the approximating solutions to the state equations and their gradients with respect to the design parameters as well as the convergence of the solutions to the resulting approximating optimal design problems to an optimal design for the original infinite dimensional device.

Practical implementations of our designs will likely exploit the fact that $V(x)$ in modern semiconductor materials such as $\text{Al}_\xi\text{Ga}_{1-\xi}\text{As}$ can be controlled with atomic layer precision in the x direction using techniques such as molecular beam epitaxy. In $\text{Al}_\xi\text{Ga}_{1-\xi}\text{As}$ the average value of local potential energy in each atomic monolayer is determined by the fraction ξ of Al. The behavior of electronic devices with layers that are a few nanometers thick may often be characterized by ballistic electron transmission probability T , as a function of applied voltage bias V_{bias} . (The precise definition of the transmission coefficient T is given in section 2).

We formulate a design problem in terms of identifying designs for $V(x)$ that result in locally optimal electron transmission characteristics $T = T(V_{\text{bias}})$. The design criterion is formulated in terms of the squared difference between the desired and observed performance of the device. We solve the optimal design problem by seeking local minima via a gradient-based search.

Although in classical optimal design there is an obvious preference for global minima, in the problem of interest to us here, we are motivated to develop highly efficient methods for identifying local minima. The parameter space can be of high dimension, and the optimization landscape can be rather complex and nonconvex. Consequently, a truly random search technique for a global optimum, such as a genetic algorithm, is likely to be untenable. A more pragmatic approach is a highly efficient local exploration of potentially promising subsets of the design space first identified by parallelized random search. In light of this, we have concentrated our efforts on developing numerically stable, convergent, and computationally efficient methods for evaluating the gradient of the performance index with respect to the design parameters.

The underlying physics of a nanoscale device are at the quantum level, and therefore the performance constraints will be described by the Schrödinger equation. When the underlying constraints involve differential equations, one typically relies on some form of finite-difference approximation to make the optimization problem amenable to numerical solution and to make use of the adjoint method to facilitate efficient and accurate computation of gradients. In such cases, careful attention must be paid to convergence and stability. For the design problem of particular interest to us here, we have developed a numerically stable and convergent reformulation and approximation of the underlying two-point boundary value problem constraints as a discrete terminal value problem that allows us to maximally exploit the power of the adjoint method for the efficient and exact (i.e., no truncation error) computation of gradients.

The optimal design of nanoscale devices of the type of interest to us here has been studied previously by different authors in [2] and [3]. The work we report on is most closely related to the effort described in [2], where an exhaustive search method was used to solve the optimization problem that results when the design problem is

formulated as a nonlinear least-squares fit to a desired performance. This approach is highly computationally intensive and hence impractical for implementation as a design tool.

In [3] the authors propose a sequential linear programming-based algorithm for finding the potential energy profile that produces the desired transmission coefficient performance in the presence of parameter uncertainty. They formulate an appropriate robust stochastic optimization problem for which their sequential linear programming scheme can be used to find locally optimal solutions. In so far as both our approach and the approach taken in [3] find local optima, it is worth noting that for the same design problem, the two schemes find similar but not identical optimal potential profiles.

A brief outline of the paper is as follows. In section 2 we define and formulate the optimal layered potential design problem of interest to us here. In particular, we present the quantum mechanical basis for the underlying physics of the devices we are interested in designing and precisely formulate the performance measure we wish to optimize in terms of the transmission function or coefficient. In section 3 we develop a finite dimensional approximation scheme for the underlying two-point boundary value problem that must be solved to evaluate the transmission function, and we show how it can be combined with a computationally efficient adjoint method for computing the analytic gradients used to find locally optimal potential profiles. In section 4 we demonstrate the numerical stability of our method, and we establish a subsequential convergence result for the sequence of approximating optimal potential profiles as the level of discretization tends to infinity. We establish the differentiability of the approximating optimal design least-squares performance indices and the convergence of their gradients. In section 5 we present the results of some of our numerical studies in which we determine locally optimal potential profiles for devices exhibiting linear, quadratic, and square root transmission characteristics. Section 6 includes some discussion of our results and a few concluding remarks.

2. The optimal design problem. We consider a layered nanoscale semiconductor electronic device schematically configured as shown in Figure 2.1. The device is assumed to be of total thickness L and to consist of N layers. For $i = 1, 2, \dots, N$, the i th layer begins and ends at positions x_{i-1} and x_i , respectively, and is of thickness $L_i = x_i - x_{i-1}$. It follows therefore that $x_N - x_0 = L$. The local potential energy in the i th barrier layer is assumed to be U_i , with $i = 1, 2, \dots, N$. For $x < x_0$, the local potential energy is assumed to be U_0 , and for $x > x_N$, it is assumed to be U_{N+1} . We assume that a single electron propagating from $-\infty$ is incident upon the left boundary of the device at x_0 and that a voltage bias V_{bias} is applied across the device.

Typically, application of the voltage bias illustrated in Figure 2.1 has the effect of creating an accumulation of charge on the left side of the barrier layers and a depletion region on the far right. Obtaining the precise form of the resulting potential energy profile $V(x)$ requires the solution of an appropriate Poisson equation [4]. However, for our purposes here, we assume that the thickness of the depletion and accumulation layers is sufficiently small so as to allow for linear approximation. Consequently, the static potential energy profile takes the form

$$(2.1) \quad V(x) = V(x; \mathbf{U}, V_{\text{bias}}) = \begin{cases} U_0, & -\infty < x < x_0, \\ \sum_{j=1}^N U_j \chi_j(x) - V_{\text{bias}} \frac{x-x_0}{L}, & x_0 \leq x \leq x_N, \\ U_{N+1} - V_{\text{bias}}, & x_N < x < \infty, \end{cases}$$

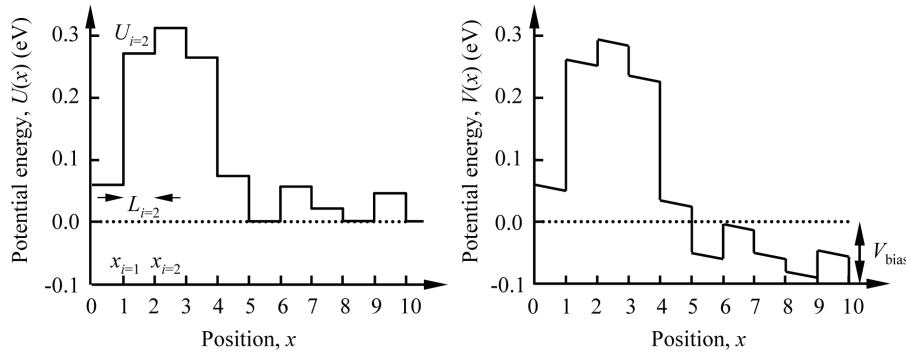


FIG. 2.1. A layered nanoscale semiconductor device (left) and the device with a bias voltage V_{bias} applied across it (right).

where $\mathbf{U} = \{U_i\}_{i=1}^N$ describes the local layer potentials. For each $j = 1, 2, \dots, N$, χ_j is the characteristic function corresponding to the j th subinterval, $[x_{j-1}, x_j]$. That is,

$$\chi_j(x) = \begin{cases} 1, & x_{j-1} \leq x < x_j, \\ 0 & \text{otherwise.} \end{cases}$$

The interaction of the electron with the potential $V(x)$ is described by solving for the electron wave function Ψ in the Schrödinger equation

$$(2.2) \quad -\frac{\hbar^2}{2m_0} \frac{\partial^2 \Psi(x, t)}{\partial x^2} + V(x) \Psi(x, t) = i\hbar \frac{\partial \Psi(x, t)}{\partial t},$$

where $\hbar = 1.05492 \times 10^{-34}$ J is Planck's constant, $m_0 = 9.10938188 \times 10^{-31}$ kg is the bare electron mass, and $\mathbf{i} = \sqrt{-1}$. In a semiconductor the bare electron mass is often replaced by an effective electron mass m^* . Charge density flux $\partial \rho_e(x, t)/\partial t$ is given by [5]

$$(2.3) \quad \begin{aligned} \frac{\partial \rho_e}{\partial t} &= \frac{\partial |\Psi|^2}{\partial t} = \frac{\partial (\bar{\Psi} \Psi)}{\partial t} = \bar{\Psi} \frac{\partial \Psi}{\partial t} + \Psi \frac{\partial \bar{\Psi}}{\partial t} \\ &= \bar{\Psi} \left\{ -\frac{\hbar}{2m_0 \mathbf{i}} \frac{\partial^2 \Psi}{\partial x^2} + \frac{1}{\mathbf{i}\hbar} V(x) \Psi \right\} + \Psi \left\{ \frac{\hbar}{2m_0 \mathbf{i}} \frac{\partial^2 \bar{\Psi}}{\partial x^2} - \frac{1}{\mathbf{i}\hbar} V(x) \bar{\Psi} \right\} \\ &= -\frac{\partial}{\partial x} \frac{\hbar}{2m_0 \mathbf{i}} \left\{ \bar{\Psi} \frac{\partial \Psi}{\partial x} - \Psi \frac{\partial \bar{\Psi}}{\partial x} \right\}, \end{aligned}$$

where unit electron charge is assumed, the potential energy function $V(x)$ is taken to be real, and we make use of the Schrödinger equation (2.2). If we define *current density* $\hat{j} = \hat{j}(x, t)$ by

$$(2.4) \quad \hat{j}(x, t) = \frac{\hbar}{2m_0 \mathbf{i}} \left\{ \bar{\Psi}(x, t) \frac{\partial \Psi(x, t)}{\partial x} - \Psi(x, t) \frac{\partial \bar{\Psi}(x, t)}{\partial x} \right\},$$

(2.3) and (2.4) together then yield the differential relation

$$(2.5) \quad \frac{\partial \rho_e}{\partial t} + \frac{\partial \hat{j}}{\partial x} = 0,$$

which is a continuity equation. In this way, (2.5) becomes a statement of conservation of current.

The transmission coefficient T of the device is then defined to be a ratio of current densities as

$$(2.6) \quad T = T(V_{\text{bias}}, \mathbf{U}) = \frac{|\hat{j}_{\text{trans}}|}{|\hat{j}_{\text{inc}}|},$$

where \hat{j}_{trans} is the current density transmitted from the device at $x = x_N$ and \hat{j}_{inc} denotes the current density incident upon the device at $x = x_0$.

Since the potential $V(x)$ is independent of time, (2.2) admits a solution of the form $\Psi(x, t) = \psi(x)\varphi(t)$ which can be found via separation of variables. The time-dependent factor, $\varphi(t)$, must satisfy the equation

$$\mathbf{i}\hbar \frac{\partial \varphi(t)}{\partial t} = E\varphi(t)$$

and is therefore given by

$$(2.7) \quad \varphi(t) = e^{-\mathbf{i}\frac{E}{\hbar}t},$$

where E , the separation constant, is the sum of electron kinetic and potential energy. For the conservative system we consider, energy E is a constant of the electron motion. The time-independent wave function $\psi(x)$ is then found as the solution to the second-order ordinary differential equation (time-independent Schrödinger equation) given by

$$(2.8) \quad -\frac{\hbar^2}{2m_0} \frac{d^2\psi(x)}{dx^2} + V(x)\psi(x) = E\psi(x).$$

With the potential $V(x)$ as given in (2.1), on the intervals $-\infty < x < x_0$ and $x_N < x < \infty$, the general solution to (2.8) is given by

$$(2.9) \quad \psi_0(x) = A_0 e^{\mathbf{i}k_0 x} + B_0 e^{-\mathbf{i}k_0 x}$$

and

$$(2.10) \quad \psi_{N+1}(x) = A_{N+1} e^{\mathbf{i}k_{N+1}(x-x_N)} + B_{N+1} e^{-\mathbf{i}k_{N+1}(x-x_N)},$$

respectively, where $k_0^2 = \frac{2m_0(E-U_0)}{\hbar^2}$, $k_{N+1}^2 = \frac{2m_0(E-U_{N+1}+V_{\text{bias}})}{\hbar^2}$, and the in general complex coefficients, A_0 , B_0 , A_{N+1} , B_{N+1} , are determined by the boundary conditions. We assume that $E > U_0$ and $E > U_{N+1} - V_{\text{bias}}$. The latter two assumptions are made to ensure that the time-independent Schrödinger equation (2.8) admits exponential solutions of the form (2.9) and (2.10) on the intervals $-\infty < x < x_0$ and $x_N < x < \infty$, respectively, as opposed to polynomial (i.e., linear) solutions. For ease of exposition and clarity, we exclusively treat the exponential case here. However, our general approach may be readily modified to handle the polynomial case as well.

Combining (2.7), (2.9), and (2.10), it is clear that for $-\infty < x < x_0$ and $x_N < x < \infty$, the time-dependent wave function $\Psi(x, t) = \psi(x)\varphi(t)$ is of the form

$$(2.11) \quad \Psi(x, t) = A_0 e^{\mathbf{i}k_0(x-\frac{E}{\hbar}t)} + B_0 e^{-\mathbf{i}k_0(x+\frac{E}{\hbar}t)}$$

and

$$(2.12) \quad \Psi(x, t) = A_{N+1} e^{ik_{N+1}(x-x_N - \frac{E}{\hbar}t)} + B_{N+1} e^{-ik_{N+1}(x-x_N + \frac{E}{\hbar}t)},$$

respectively. In this way, the wave function can be viewed as the sum of left and right propagating wave amplitudes. Moreover, as a result of the significant likelihood of reflection at interfaces across which there is a significant change in the electron's velocity, it is clear that the second term in (2.11) and the first term in (2.12) represent the cumulative sum of the interference effects that result from, respectively, the reflected and the transmitted amplitude at each change in the spatial potential $V(x)$ of the device.

With the time-dependent wave function on the intervals $-\infty < x < x_0$ and $x_N < x < \infty$ written in the form of (2.11) and (2.12) it is now straightforward to identify the relevant boundary conditions and to obtain an explicit expression for the transmission coefficient T given in (2.6). Indeed, it is immediately clear that $|A_0|$ is the amplitude of the electron wave function impinging on the left boundary of the device at $x = x_0$. Hence, for an electron incident from the left, $|A_0|^2 = 1$, and since there is neither transmission nor reflection from $x = +\infty$ we require $B_{N+1} = 0$. Furthermore, from (2.4), (2.11), and (2.12), an easy calculation yields the following expressions for the transmitted and incident current densities:

$$(2.13) \quad \hat{j}_{\text{trans}} = \frac{\hbar k_{N+1}}{m_0} |A_{N+1}|^2 \quad \text{and} \quad \hat{j}_{\text{inc}} = \frac{\hbar k_0}{m_0} |A_0|^2.$$

Combining (2.6) and (2.13), we immediately obtain

$$(2.14) \quad T = T(V_{\text{bias}}) = T(V_{\text{bias}}, \mathbf{U}) = \frac{k_{n+1} |A_{N+1}|^2}{k_0 |A_0|^2}.$$

A typical design problem might involve determining layer potentials, U_i , with $i = 1, 2, \dots, N$, which yield power law-like transmission characteristics. For example, if one desired an essentially ohmic response, one would seek layer potentials that produce a transmission function that is linear over a specified range of bias voltages, $V_{\text{min}} \leq V_{\text{bias}} \leq V_{\text{max}}$. Other design problems of interest might involve, for example, finding layer potentials which yield either quadratic or square root transmission characteristics over specified intervals of bias voltages.

As an initial approach, we formulate the optimal design problem mathematically as a constrained least-squares fit to a given desired transmission function $T_0 = T_0(V_{\text{bias}})$ defined on the interval $V_{\text{min}} \leq V_{\text{bias}} \leq V_{\text{max}}$. More precisely we seek local layer potentials $\mathbf{U} = \{U_i\}_{i=1}^N$, with $U_L \leq U_i \leq U_H$ and $i = 1, 2, \dots, N$, which minimize the least-squares functional

$$(2.15) \quad J(\mathbf{U}) = \sum_{j=1}^{\nu} |T_0(V_j) - T(V_j, \mathbf{U})|^2,$$

where $T = T(V_j; \mathbf{U})$ is given by (2.14) with $V_{\text{bias}} = V_j$, and $V_{\text{min}} \leq V_j \leq V_{\text{max}}$, $j = 1, 2, \dots, \nu$, are given arbitrarily spaced bias voltages in the interval $[V_{\text{min}}, V_{\text{max}}]$.

3. Solving the optimal design problem and the adjoint method. The optimal design problem formulated as a least-squares fit to data will be solved numerically by finding local minima via gradient-based steepest descent or Newton's

methods. To do this we require accurate and computationally efficient ways to calculate $T(V_{\text{bias}}, \mathbf{U})$ at $V_{\text{bias}} = V_j$ and \mathbf{U} , and the gradient of the performance index J given by (2.15), $\nabla J(\mathbf{U})$, for a given choice of \mathbf{U} . Following the development in section 2, we seek solutions to the time-independent Schrödinger equation given in (2.8) on $(-\infty, \infty)$ which are smooth (i.e., C^1) across the device boundaries at $x = x_0$ and $x = x_N$. That is, we seek solutions $\psi = \psi(x)$, $-\infty < x < \infty$, to (2.8) satisfying the boundary conditions

$$\psi(x_0) = \psi_0(x_0), \quad \psi'(x_0) = \psi'_0(x_0),$$

$$\psi(x_N) = \psi_{N+1}(x_N), \quad \psi'(x_N) = \psi'_{N+1}(x_N),$$

where the functions ψ_0 and ψ_{N+1} are given by (2.9) and (2.10), respectively. Recalling that the interpretation of (2.9) and (2.10) as the sum of forward and backward propagating waves implies that $B_{N+1} = 0$, the two conditions given above at $x = x_0$ can be combined to eliminate the constant of integration B_0 , and the two conditions given above at $x = x_N$ can be combined to eliminate the constant of integration A_{N+1} , yielding the linear second-order two-point boundary value problem on $[x_0, x_N]$ parameterized by A_0 given by

$$(3.1) \quad -\frac{\hbar^2}{2m_0} \frac{d^2\psi(x)}{dx^2} + V(x)\psi(x) = E\psi(x), \quad x_0 < x < x_N,$$

$$(3.2) \quad \mathbf{i}k_0\psi(x_0) + \psi'(x_0) = 2\mathbf{i}k_0A_0e^{\mathbf{i}k_0x_0},$$

$$(3.3) \quad \mathbf{i}k_{N+1}\psi(x_N) - \psi'(x_N) = 0.$$

Then if ψ is the solution to (3.1)–(3.3) on the interval $[x_0, x_N]$, the desired solution on $(-\infty, \infty)$ can then be obtained by combining ψ on $[x_0, x_N]$ with ψ_0 on $(-\infty, x_0]$ and ψ_{N+1} on $[x_N, \infty)$ given by (2.9) and (2.10), respectively, with $A_{N+1} = \psi(x_N)$ and $B_0 = e^{\mathbf{i}k_0x_0}\psi(x_0) - A_0e^{2\mathbf{i}k_0x_0}$. It then follows that $A_{N+1} = \psi(x_N) = \psi(x_N; A_0) = A_0\psi(x_N; 1)$ is linear in A_0 and, moreover, that the value of $T(V_{\text{bias}}, \mathbf{U})$ is independent of the value of A_0 . Indeed, in light of (2.14), it follows that $T(V_{\text{bias}}) = T(V_{\text{bias}}, \mathbf{U}) = \frac{|A_{N+1}|^2 k_{N+1}}{|A_0|^2 k_0} = \frac{k_{N+1} |\psi(x_N; A_0)|^2}{k_0 |A_0|^2} = \frac{k_{N+1}}{k_0} |\psi(x_N; 1)|^2 = \frac{k_{N+1}}{k_0} |\psi(x_N; V_{\text{bias}}, \mathbf{U})|^2$, where $\psi(\cdot; V_{\text{bias}}, \mathbf{U})$ denotes the solution to the two-point boundary value problem (3.1)–(3.3) corresponding to $V_{\text{bias}}, A_0 = 1$, and $\mathbf{U} = \{U_i\}_{i=1}^N$. Then, recalling (2.15), solving the optimal design problem requires the minimization of the least-squares functional

$$(3.4) \quad J(\mathbf{U}) = \sum_{j=1}^{\nu} \left| T_0(V_j) - \frac{k_{N+1,j}}{k_0} |\psi(x_N; V_j, \mathbf{U})|^2 \right|^2,$$

where $\psi(\cdot, V_j, \mathbf{U})$ is the solution to the two-point boundary value problem (3.1)–(3.3) corresponding to $V_{\text{bias}} = V_j, j = 1, 2, \dots, \nu, A_0 = 1$, and $\mathbf{U} = \{U_i\}_{i=1}^N$, and we have added the subscript j to k_{N+1} to reflect the fact that $k_{N+1}^2 = \frac{2m_0(E - U_{N+1} + V_{\text{bias}})}{\hbar^2}$ depends on the value of the bias voltage V_{bias} . That is, for $j = 1, 2, \dots, \nu, k_{N+1,j}^2 = \frac{2m_0(E - U_{N+1} + V_j)}{\hbar^2}$.

3.1. Approximation. Actually solving the least-squares minimization problem requires that we be able to numerically solve (3.1)–(3.3). In what follows, we propose a numerical scheme based on an idea known as the propagation method (see, for example, [6]) that approximates the second-order linear ordinary differential equation–based two-point boundary value problem by a two-point boundary value problem for a two-dimensional linear nonautonomous difference equation. Then by using the linear relationship that exists between A_{N+1} and A_0 together with the fact that the transmission function is the quotient of A_{N+1} and A_0 , we are able to replace the boundary value problem by the much more easily solved terminal value problem. This in turn permits the highly accurate and efficient computation of the gradient of J via the adjoint method.

Toward this end, for each $M = 1, 2, \dots$, we partition each of the layers $[x_{j-1}, x_j]$, $j = 1, 2, \dots, N$, into M equal sublayers, $[x_{(j-1)M+m-1}^M, x_{(j-1)M+m}^M]$, with $m = 1, 2, \dots, M$, $x_0^M = x_0$, and $x_{(j-1)M+m}^M = x_{j-1} + \frac{mL_j}{M}$, $j = 1, 2, \dots, N$, and $m = 1, 2, \dots, M$. We then consider the time-independent Schrödinger equation (2.8) with the potential function V given by (2.1) replaced by the piecewise constant approximation V^M given by

$$(3.5) \quad V^M(x) = V\left(x_{(j-1)M+m-1}^M\right), \quad x_{(j-1)M+m-1}^M \leq x < x_{(j-1)M+m}^M,$$

$j = 1, 2, \dots, N$ and $m = 1, 2, \dots, M$. For $\mathbf{U} = \{U_i\}_{i=1}^N$ and V_{bias} given, and $j = 1, 2, \dots, N$ and $m = 1, 2, \dots, M$, we set

$$(3.6) \quad \left[k_{(j-1)M+m}^M\right]^2 = \frac{2m_0}{\hbar^2} \left(E - U_j + V_{\text{bias}} \frac{x_{(j-1)M+m-1}^M - x_0}{L} \right),$$

$k_0^M = k_0$, and $k_{NM+1}^M = k_{N+1}$.

Then, for $j = 1, 2, \dots, N$ and $m = 1, 2, \dots, M$, on the interval $[x_{(j-1)M+m-1}^M, x_{(j-1)M+m}^M]$, the general solution to the time-independent Schrödinger equation with V replaced by V^M is given by

$$\begin{aligned} \psi_{(j-1)M+m}^M(x) &= A_{(j-1)M+m}^M e^{ik_{(j-1)M+m}^M(x-x_{(j-1)M+m-1}^M)} \\ &\quad + B_{(j-1)M+m}^M e^{-ik_{(j-1)M+m}^M(x-x_{(j-1)M+m-1}^M)}, \end{aligned}$$

where $A_{(j-1)M+m}^M$ and $B_{(j-1)M+m}^M$ in the above expressions are arbitrary constants of integration. We also set $\psi_0^M = \psi_0$ and $\psi_{NM+1}^M = \psi_{N+1}$, where ψ_0 and ψ_{N+1} are given by (2.9) and (2.10), respectively. Once again, for ease of exposition, we have assumed that E , the sum of electron kinetic and potential energy; the layer potentials, $\mathbf{U} = \{U_i\}_{i=1}^N$; and bias voltages, V_{bias} , are such that the time-independent Schrödinger equation (2.8) with V replaced by V^M admits an exponential solution of the form given above on each subinterval $[x_{(j-1)M+m-1}^M, x_{(j-1)M+m}^M]$. As before, our approach is easily modified to handle the polynomial case as well.

We seek a smooth (i.e., C^1) solution on $[x_0, x_N]$. Consequently, by setting

$$\begin{aligned} \psi_{(j-1)M+m}^M\left(x_{(j-1)M+m}^M\right) &= \psi_{(j-1)M+m+1}^M\left(x_{(j-1)M+m}^M\right), \\ \frac{d\psi_{(j-1)M+m}^M}{dx}\left(x_{(j-1)M+m}^M\right) &= \frac{d\psi_{(j-1)M+m+1}^M}{dx}\left(x_{(j-1)M+m}^M\right), \end{aligned}$$

$\psi_0^M(x_0^M) = \psi_1^M(x_0^M)$, $d\psi_0^M/dx(x_0^M) = d\psi_1^M/dx(x_0^M)$, $L_{(j-1)M+m}^M = x_{(j-1)M+m}^M - x_{(j-1)M+m-1}^M = \frac{L_j}{M}$ for $j = 1, 2, \dots, N$ and $m = 1, 2, \dots, M$, and $L_0^M = x_0^M$, we obtain the system of equations given in matrix form by

$$(3.7) \quad \begin{bmatrix} e^{ik_n^M L_n^M} & e^{-ik_n^M L_n^M} \\ ik_n^M e^{ik_n^M L_n^M} & -ik_n^M e^{-ik_n^M L_n^M} \end{bmatrix} \begin{bmatrix} A_n^M \\ B_n^M \end{bmatrix} = \begin{bmatrix} 1 & 1 \\ ik_{n+1}^M & -ik_{n+1}^M \end{bmatrix} \begin{bmatrix} A_{n+1}^M \\ B_{n+1}^M \end{bmatrix},$$

where $n = 0, 1, 2, \dots, NM$. Alternatively, inverting the 2×2 matrix on the left-hand side of (3.7), one obtains

$$(3.8) \quad \begin{bmatrix} A_n^M \\ B_n^M \end{bmatrix} = \frac{1}{2} \begin{bmatrix} \left(1 + \frac{k_{n+1}^M}{k_n^M}\right) e^{-ik_n^M L_n^M} & \left(1 - \frac{k_{n+1}^M}{k_n^M}\right) e^{-ik_n^M L_n^M} \\ \left(1 - \frac{k_{n+1}^M}{k_n^M}\right) e^{ik_n^M L_n^M} & \left(1 + \frac{k_{n+1}^M}{k_n^M}\right) e^{ik_n^M L_n^M} \end{bmatrix} \begin{bmatrix} A_{n+1}^M \\ B_{n+1}^M \end{bmatrix} \\ \equiv \mathbf{P}_n^M(\mathbf{U}, V_{\text{bias}}) \begin{bmatrix} A_{n+1}^M \\ B_{n+1}^M \end{bmatrix},$$

$n = 0, 1, 2, \dots, NM$. With the incident electron of amplitude $|A_0|$ being introduced on the left and no reflective wave propagating to the left from $+\infty$, we also have the two boundary conditions

$$(3.9) \quad \begin{bmatrix} 1 & 0 \end{bmatrix} \begin{bmatrix} A_0^M \\ B_0^M \end{bmatrix} = A_0 \quad \text{and} \quad \begin{bmatrix} 0 & 1 \end{bmatrix} \begin{bmatrix} A_{NM+1}^M \\ B_{NM+1}^M \end{bmatrix} = 0.$$

The least-squares performance indices for the approximating optimal design problem then become

$$(3.10) \quad J^M(\mathbf{U}) = \sum_{j=1}^{\nu} \left| T_0(V_j) - \frac{|A_{NM+1}^M(V_j, \mathbf{U})|^2 k_{N+1,j}}{|A_0^M|^2 k_0} \right|^2 \\ = \sum_{j=1}^{\nu} \left| T_0(V_j) - \frac{|A_{NM+1}^M(V_j, \mathbf{U})|^2 k_{N+1,j}}{|A_0|^2 k_0} \right|^2,$$

where, as before, for $j = 1, 2, \dots, \nu$, $k_{N+1,j}$ is defined by $k_{N+1,j}^2 = \frac{2m_0(E-U_{N+1}+V_j)}{\hbar^2}$. Once again we observe that A_{NM+1}^M depends linearly on A_0 and consequently on A_0^M as well. It follows that the value of

$$T^M(V_{\text{bias}}) = T^M(V_{\text{bias}}, \mathbf{U}) = |A_{NM+1}^M|^2 k_{N+1} / |A_0^M|^2 k_0$$

is independent of the value of A_0 . Moreover, it necessarily follows that A_0^M depends linearly on A_{NM+1}^M and that the value of

$$T^M(V_{\text{bias}}) = T^M(V_{\text{bias}}, \mathbf{U}) = |A_{NM+1}^M|^2 k_{N+1} / |A_0^M|^2 k_0$$

is independent of the value of A_{NM+1}^M if it is specified instead of A_0^M . It follows that, without affecting the solution to the optimal design problem and without loss of generality, we may set $A_{NM+1}^M = 1$. The boundary conditions given in (3.9) can then be replaced with the single terminal condition

$$(3.11) \quad \begin{bmatrix} A_{NM+1}^M \\ B_{NM+1}^M \end{bmatrix} = \begin{bmatrix} 1 \\ 0 \end{bmatrix},$$

and the least-squares performance indices given in (3.10) can be replaced by

$$(3.12) \quad J^M(\mathbf{U}) = \sum_{j=1}^{\nu} \left| T_0(V_j) - \frac{k_{N+1,j}}{|A_0^M(V_j, \mathbf{U})|^2 k_0} \right|^2.$$

Solving the approximating optimal design problem then consists of finding local layer potentials $\mathbf{U}^* = \{U_i^*\}_{i=1}^N$ which minimize the least-squares performance index (3.12) subject to the system of two linear difference equations (3.8) and the terminal condition (3.11).

3.2. The adjoint method. The formulation of the optimal design problem as the minimization of a least-squares performance index subject to a terminal value problem for a system of linear difference equations lends itself extremely well to efficient and accurate (in fact, no truncation error) gradient calculation via the adjoint method. The adjoint method has its roots in the classical theory of constrained optimization, Lagrange multipliers, and optimal control. Associated with and coupled to the constraints on the system state variables is another, related, system of equations known as the adjoint. In this context, the adjoint system is most familiar for the role it plays in the formulation of necessary conditions for optimality as given in what is generally regarded as the fundamental theorem of optimal control, the Pontryagin maximum principle (see, for example, [7], [8]), a dynamic version of the method of Lagrange multipliers from elementary calculus. The adjoint is typically a dynamical system that is of a similar form to the state equation, typically an ordinary differential or difference equation (see, for example, [9] and [10]) or even a partial differential equation (see, for example, [11]). The variables in the adjoint system are known as the costates, dual variables, or Lagrange multipliers, and they describe the propagation of a hyperplane characterized by a normal that is related to the tangent to the curve determined by the state trajectory [12]. At optimality, the costate variables may be interpreted as the marginal benefit derived (with respect to the underlying performance index being optimized) by weakening the constraints on the state variables. In fact, they are sensitivities and are related to various derivatives of the cost functional. Economists sometimes refer to them as either *imputed* or *shadow prices*. However, it turns out that at nonstationary points, the adjoint may also be used to facilitate the highly efficient computation of the gradient of the performance index with respect to the optimization parameters. In essence, it does this by making it unnecessary to directly compute derivatives of the state variables with respect to the optimization parameters. This computational *sleight of hand* is more or less unrelated to the role played by the adjoint in optimal control theory and is actually realized through a relatively simple combination of elementary calculus and linear duality (see [13]). Indeed, to see how this works in its most general form, consider the computation of the gradient of the performance index $J(\mathbf{q}) = F(\mathbf{x}(\mathbf{q}))$ subject to the in general nonlinear system $\mathbf{G}(\mathbf{q}, \mathbf{x}) = \mathbf{0}$, where the design parameters are $\mathbf{q} \in \mathbf{R}^p$, the state is given by $\mathbf{x} \in \mathbf{R}^n$, \mathbf{G} is an \mathbf{R}^n -valued differentiable function on $\mathbf{R}^p \times \mathbf{R}^n$, and F is a real-valued differentiable function on \mathbf{R}^n . We note that, without any loss of generality, it is entirely sufficient to consider the adjoint method only for this static state equation $\mathbf{G}(\mathbf{q}, \mathbf{x}) = \mathbf{0}$ since the case of a constraint given by a discrete-time dynamical system (in particular, including the one in the previous section) can readily be put into this general form.

Using the chain rule to differentiate the performance index and the state equation

with respect to \mathbf{q} , we obtain the two expressions

$$\nabla J(\mathbf{q}) = \nabla F(\mathbf{x}(\mathbf{q})) \frac{\partial \mathbf{x}}{\partial \mathbf{q}} \quad \text{and} \quad \frac{\partial \mathbf{G}(\mathbf{q}, \mathbf{x})}{\partial \mathbf{x}} \frac{\partial \mathbf{x}}{\partial \mathbf{q}} = -\frac{\partial \mathbf{G}(\mathbf{q}, \mathbf{x})}{\partial \mathbf{q}}.$$

Now it appears that in order to evaluate $\nabla J(\mathbf{q})$, the p linear systems given in the expression on the right will have to be solved for $\partial \mathbf{x} / \partial \mathbf{q}$ (for simplicity, we assume here that the matrix $\partial \mathbf{G}(\mathbf{q}, \mathbf{x}) / \partial \mathbf{x}$ is nonsingular). However, this is in fact not the case. Indeed, note that the expression on the right indicates that the columns of $\partial \mathbf{x} / \partial \mathbf{q}$ are actually the vector representations for the columns of the matrix $-\partial \mathbf{G}(\mathbf{q}, \mathbf{x}) / \partial \mathbf{q}$ with respect to the basis defined by the columns of $\partial \mathbf{G}(\mathbf{q}, \mathbf{x}) / \partial \mathbf{x}$. Consequently, we consider the linear functional on \mathbf{R}^n given by $\ell(\mathbf{y}) = \langle \nabla F(\mathbf{x}(\mathbf{q})), \mathbf{y} \rangle$ with $\nabla F(\mathbf{x}(\mathbf{q})) \in \mathbf{R}^{1 \times n}$ being its matrix representation with respect to the basis defined by the columns of $\partial \mathbf{G}(\mathbf{q}, \mathbf{x}) / \partial \mathbf{x}$. Then, if instead we determine $\mathbf{z}^T \in \mathbf{R}^{1 \times n}$ as its matrix representation with respect to the standard basis on \mathbf{R}^n via the equations

$$z_i = \ell(\mathbf{e}_i) = \langle \nabla F(\mathbf{x}(\mathbf{q})), \mathbf{e}_i \rangle = \nabla F(\mathbf{x}(\mathbf{q})) (\partial \mathbf{G}(\mathbf{q}, \mathbf{x}) / \partial \mathbf{x})^{-1} \mathbf{e}_i,$$

with $i = 1, 2, \dots, n$ and where \mathbf{e}_i denotes the i th standard basis element, or, equivalently, by solving the single linear system known as the adjoint, costate, or dual system given by $(\partial \mathbf{G}(\mathbf{q}, \mathbf{x}) / \partial \mathbf{x})^T \mathbf{z} = \nabla F(\mathbf{x}(\mathbf{q}))^T$ for \mathbf{z} , then the gradient of J , $\nabla J(\mathbf{q})$, can then be evaluated via

$$\nabla J(\mathbf{q}) = \nabla F(\mathbf{x}(\mathbf{q})) \frac{\partial \mathbf{x}}{\partial \mathbf{q}} = -\mathbf{z}^T \frac{\partial \mathbf{G}(\mathbf{q}, \mathbf{x})}{\partial \mathbf{q}}.$$

This yields a realized savings of now having to solve only two systems, the in general nonlinear state equation for \mathbf{x} and the linear adjoint or costate system for \mathbf{z} , rather than one nonlinear system and p linear systems. Even though all p systems involve the same system matrix, when this computation is inside an optimization loop, the savings due to the use of the adjoint can be significant. When the adjoint formulation for computing the gradient is applied in the context of dynamical rather than static constraints and when we take advantage of the resulting highly specialized structure of the matrices involved, the savings can be even more impressive. Note also the benefits derived from the adjoint method when compared to a more naïve finite-difference approach which would entail the solution of $p + 1$ nonlinear systems and the introduction of truncation error every time the gradient $\nabla J(\mathbf{q})$ is computed.

To see how the adjoint method is realized in the context of the optimal design problem of interest to us here, we rewrite the underlying system of difference equations (3.8) and the terminal condition (3.11) as

$$(3.13) \quad \alpha_{i,j} = \mathbf{P}_{i,j} \alpha_{i+1,j} \quad \text{and} \quad \alpha_{NM+1,j} = \begin{bmatrix} 1 \\ 0 \end{bmatrix},$$

where for $j = 1, 2, \dots, \nu$ and $i = 0, 1, 2, \dots, NM$, $\mathbf{P}_{i,j} = \mathbf{P}_i^M(\mathbf{U}, V_j)$ and $\alpha_{i,j} = [A_i^M, B_i^M]^T = [A_i^M(\mathbf{U}, V_j), B_i^M(\mathbf{U}, V_j)]^T$. The least-squares performance index (3.12) is then given by

$$(3.14) \quad J^M(\mathbf{U}) = \sum_{j=1}^{\nu} \left| T_0(V_j) - \frac{k_{N+1,j}}{|\mathbf{c}\alpha_{0,j}|^2 k_0} \right|^2 = \sum_{j=1}^{\nu} \left| T_0(V_j) - \frac{k_{N+1,j}}{\bar{\alpha}_{0,j}^T \mathbf{Q} \alpha_{0,j} k_0} \right|^2,$$

where $\mathbf{c} = [1, 0]$ and $\mathbf{Q} = \mathbf{c}^T \mathbf{c} = \begin{bmatrix} 1 & 0 \\ 0 & 0 \end{bmatrix}$. We define the adjoint or costate system corresponding to (3.13) and (3.14) as the initial value problem given by

$$\beta_{i+1,j} = \mathbf{P}_{i-1,j}^T \beta_{i,j} + \delta_{i0} 4 \left[T_0(V_j) - \frac{k_{N+1,j}}{\bar{\alpha}_{i,j}^T \mathbf{Q} \alpha_{i,j} k_0} \right] \frac{\mathbf{Q} \bar{\alpha}_{i,j} k_{N+1,j}}{(\bar{\alpha}_{i,j}^T \mathbf{Q} \alpha_{i,j})^2 k_0}$$

and $\beta_{0,j} = 0$, where δ_{ij} denotes the Kronecker delta function. It then follows that

$$\begin{aligned} \nabla J^M(\mathbf{U}) &= \frac{\partial J^M}{\partial \mathbf{U}} = \sum_{j=1}^{\nu} 2 \left[T_0(V_j) - \frac{k_{N+1,j}}{\bar{\alpha}_{0,j}^T \mathbf{Q} \alpha_{0,j} k_0} \right] \frac{2 \operatorname{Re} \bar{\alpha}_{0,j}^T \mathbf{Q} \frac{\partial \alpha_{0,j}}{\partial \mathbf{U}} k_{N+1,j}}{(\bar{\alpha}_{0,j}^T \mathbf{Q} \alpha_{0,j})^2 k_0} \\ &= \operatorname{Re} \sum_{j=1}^{\nu} \sum_{i=0}^{NM} 4 \delta_{i0} \left[T_0(V_j) - \frac{k_{N+1,j}}{\bar{\alpha}_{i,j}^T \mathbf{Q} \alpha_{i,j} k_0} \right] \frac{\bar{\alpha}_{i,j}^T \mathbf{Q} k_{N+1,j}}{(\bar{\alpha}_{i,j}^T \mathbf{Q} \alpha_{i,j})^2 k_0} \frac{\partial \alpha_{i,j}}{\partial \mathbf{U}} \\ &= \operatorname{Re} \sum_{j=1}^{\nu} \sum_{i=0}^{NM} \left(\beta_{i+1,j} - \mathbf{P}_{i-1,j}^T \beta_{i,j} \right)^T \frac{\partial \alpha_{i,j}}{\partial \mathbf{U}} \\ &= \operatorname{Re} \sum_{j=1}^{\nu} \left\{ \sum_{i=0}^{NM} \beta_{i+1,j}^T \frac{\partial \alpha_{i,j}}{\partial \mathbf{U}} - \sum_{i=1}^{NM} \beta_{i,j}^T \mathbf{P}_{i-1,j} \frac{\partial \alpha_{i,j}}{\partial \mathbf{U}} \right\} \\ &= \operatorname{Re} \sum_{j=1}^{\nu} \left\{ \sum_{i=0}^{NM} \beta_{i+1,j}^T \left(\mathbf{P}_{i,j} \frac{\partial \alpha_{i+1,j}}{\partial \mathbf{U}} + \frac{\partial \mathbf{P}_{i,j}}{\partial \mathbf{U}} \alpha_{i+1,j} \right) - \sum_{i=1}^{NM} \beta_{i,j}^T \mathbf{P}_{i-1,j} \frac{\partial \alpha_{i,j}}{\partial \mathbf{U}} \right\} \\ &= \operatorname{Re} \sum_{j=1}^{\nu} \sum_{i=0}^{NM} \beta_{i+1,j}^T \frac{\partial \mathbf{P}_{i,j}}{\partial \mathbf{U}} \alpha_{i+1,j}, \end{aligned}$$

where, in light of the terminal condition given in (3.13), we have used the fact that $\frac{\partial \alpha_{NM+1,j}}{\partial \mathbf{U}} = \mathbf{0}$. Consequently, the gradient of J^M can be obtained with no truncation error according to the following steps.

1. For each $j = 1, 2, \dots, \nu$, solve the terminal value problem

$$\begin{aligned} \begin{bmatrix} A_i^M \\ B_i^M \end{bmatrix} &= \mathbf{P}_i^M(\mathbf{U}, V_j) \begin{bmatrix} A_{i+1}^M \\ B_{i+1}^M \end{bmatrix}, \\ \begin{bmatrix} A_{NM+1}^M \\ B_{NM+1}^M \end{bmatrix} &= \begin{bmatrix} 1 \\ 0 \end{bmatrix}, \\ &i = NM, NM - 1, \dots, 2, 1, 0. \end{aligned} \tag{3.15}$$

2. For each $j = 1, 2, \dots, \nu$, solve the initial value problem

$$\begin{aligned} \beta_{i+1,j} &= \mathbf{P}_i^M(\mathbf{U}, V_j)^T \beta_{i,j}, \\ \beta_{1,j} &= 4 \left[T_0(V_j) - \frac{k_{N+1,j}}{|A_0^M|^2 k_0} \right] \frac{k_{N+1,j}}{|A_0^M|^4 k_0} \begin{bmatrix} \bar{A}_0^M \\ 0 \end{bmatrix}, \\ &i = 1, 2, \dots, NM. \end{aligned} \tag{3.16}$$

3. Compute the gradient of J^M as

$$\nabla J^M(\mathbf{U}) = \operatorname{Re} \sum_{j=1}^{\nu} \sum_{i=0}^{NM} \beta_{i+1,j}^T \frac{\partial \mathbf{P}_i^M(\mathbf{U}, V_j)}{\partial \mathbf{U}} \begin{bmatrix} A_{i+1,j}^M \\ B_{i+1,j}^M \end{bmatrix}.$$

4. Numerical stability, differentiability, and convergence. Fundamental to the approach outlined above are the replacement and approximation of the two-point boundary problem given either in (3.1)–(3.3) or in (3.8), (3.9) with the initial or, more accurately, terminal value problem given by (3.8), (3.11). The solution of the optimal design problem via the adjoint method then requires the iterative sequential integration of the terminal value problem given in (3.15) for the system *state* and the adjoint initial value problem given in (3.16) for the system *costate*. As is the case when one solves a two-point boundary value problem using a shooting method that requires the iterative numerical integration of a sequence of discretized initial value problems, caution must be exercised to ensure that one has not sacrificed the inherent *numerical stability* (error remains bounded uniformly with respect to the level of discretization over the course of the computation) of solving a boundary value problem for the potential numerical instability of integrating a sequence of successively more highly discretized initial value problems. In the first part of this section, we show that the approximation scheme proposed above is indeed numerically stable.

The solutions to the recursions given in (3.15) and (3.16) are given by

$$\begin{bmatrix} A_k^M \\ B_k^M \end{bmatrix} = \left[\prod_{i=k}^{NM} \mathbf{P}_i^M(\mathbf{U}, V_j) \right] \begin{bmatrix} 1 \\ 0 \end{bmatrix}, \\ k = NM, NM - 1, \dots, 2, 1, 0,$$

and by

$$\beta_{k,j} = \left[\prod_{i=k-2}^0 \mathbf{P}_i^M(\mathbf{U}, V_j)^T \right] \beta_{1,j}, \\ \beta_{1,j} = 4 \left[T_0(V_j) - \frac{k_{N+1,j}}{|A_0^M|^2 k_0} \right] \frac{k_{N+1,j}}{|A_0^M|^4 k_0} \begin{bmatrix} \bar{A}_0^M \\ 0 \end{bmatrix}, \\ i = 1, 2, \dots, NM + 1,$$

respectively. Numerical stability will follow if we can demonstrate the boundedness of the matrix product

$$\prod_{i=0}^{NM} \mathbf{P}_i^M(\mathbf{U}, V_j)$$

uniformly in M in some appropriate matrix norm, where the matrices $\mathbf{P}_i^M(\mathbf{U}, V_j)$ are given by (3.8). Our numerical stability arguments will require the following technical assumption on the device parameters guaranteeing that the time-independent Schrödinger equation (2.8) with V replaced by V^M admits exponential solutions on each of the approximating subintervals and, moreover, that these solutions remain bounded away from becoming polynomial on any subinterval as the discretization level tends to infinity.

ASSUMPTION 4.1. *The total energy E , the layer potentials $\mathbf{U} = \{U_i\}_{i=1}^N$, the overall length of the device L , and the bias voltage V_{bias} are such that there exists a constant $\delta > 0$ for which $0 < \delta \leq |k_j^M|$, $j = 0, 1, 2, \dots, NM + 1$, where the k_j^M , $j = 1, 2, \dots, NM$, are given by (3.6), and $k_0^M = k_0$ and $k_{NM+1}^M = k_{N+1}$.*

It is not difficult to specify readily verifiable sufficient conditions needed for Assumption 4.1 to hold. Indeed, one requires only that $U_j \notin [E + \min(0, V_{\text{bias}}),$

$E + \max(0, V_{\text{bias}}]$, $j = 1, 2, \dots, N$. In the context of the optimal design problem, Assumption 4.1 will hold throughout the iterative solution procedure if the feasible set of layer potentials $[U_L, U_H]$ is chosen and the respective lower and upper bounds for the bias voltages over which the device functionality is desired, V_{min} and V_{max} , are such that $[U_L, U_H] \cap [E + \min(0, V_{\text{min}}), E + \max(0, V_{\text{max}})] = \emptyset$. With this condition, it is now straightforward to specify any number of devices and optimal design problems for which Assumption 4.1 is satisfied.

On the other hand, if the optimal design problem of interest is such that this condition cannot be met, then not only can we not verify Assumption 4.1 and therefore guarantee the numerical stability of the method, but it may in fact occur that one or more of the k_j^M given in (3.6) will vanish. In this latter case the time-independent Schrödinger equation (2.8) with V replaced by V^M has a polynomial solution on the corresponding approximating subinterval, and the system of equations given in (3.7) is no longer valid. In this case an analogous but different system of equations results, and, at least formally, the method can be appropriately modified and implemented in a similar fashion. However, the question of numerical stability of the method remains open. In this case, solving the boundary value problem (3.1)–(3.3) for the time-independent Schrödinger equation with V replaced by V^M while making sure to take advantage of the underlying structure of the problem (see (5.4)–(5.10) below) may be a better approach. Indeed, in the next section in Theorems 4.8 and 4.9 we establish convergence. However, it is worth noting that in the examples we treat in section 5 below, the sufficient condition given above that is required to establish that Assumption 4.1 is satisfied is in fact not met. Nevertheless, in all of our numerical studies we did not observe any evidence or indication of numerical instability.

LEMMA 4.1. *For $j \neq 0, M, 2M, 3M, \dots, NM$, there exists a positive constant ρ which depends on $E, \mathbf{U} = \{U_i\}_{i=1}^N$, and V_{bias} for $V_{\text{min}} \leq V_{\text{bias}} \leq V_{\text{max}}$, but which is independent of j and M such that $\|\mathbf{P}_j^M(\mathbf{U}, V_{\text{bias}})\| \leq e^{\rho \frac{L}{M}} \left(1 + \frac{2m_0 \|V_{\text{bias}}\|}{h^2 \delta^2 M}\right)^{\frac{1}{2}}$, where the constant $\delta > 0$ is as defined in Assumption 4.1 and where for a complex matrix \mathbf{A} , the matrix norm $\|\mathbf{A}\|$ is the spectral norm given by $\|\mathbf{A}\| = \sqrt{\lambda_{\text{max}}(\mathbf{A}^* \mathbf{A})}$.*

Proof. We begin by writing

$$\begin{aligned} \mathbf{P}_j^M(\mathbf{U}, V_{\text{bias}}) &= \frac{1}{2} \begin{bmatrix} \left(1 + \frac{k_{j+1}^M}{k_j^M}\right) e^{-ik_j^M L_j^M} & \left(1 - \frac{k_{j+1}^M}{k_j^M}\right) e^{-ik_j^M L_j^M} \\ \left(1 - \frac{k_{j+1}^M}{k_j^M}\right) e^{ik_j^M L_j^M} & \left(1 + \frac{k_{j+1}^M}{k_j^M}\right) e^{ik_j^M L_j^M} \end{bmatrix} \\ &= \begin{bmatrix} e^{-ik_j^M L_j^M} & 0 \\ 0 & e^{ik_j^M L_j^M} \end{bmatrix} \begin{bmatrix} \frac{1}{2} \left(1 + \frac{k_{j+1}^M}{k_j^M}\right) & \frac{1}{2} \left(1 - \frac{k_{j+1}^M}{k_j^M}\right) \\ \frac{1}{2} \left(1 - \frac{k_{j+1}^M}{k_j^M}\right) & \frac{1}{2} \left(1 + \frac{k_{j+1}^M}{k_j^M}\right) \end{bmatrix} \\ &= \begin{bmatrix} e^{-ik_j^M L_j^M} & 0 \\ 0 & e^{ik_j^M L_j^M} \end{bmatrix} \begin{bmatrix} \frac{1+\gamma_j^M}{2} & \frac{1-\gamma_j^M}{2} \\ \frac{1-\gamma_j^M}{2} & \frac{1+\gamma_j^M}{2} \end{bmatrix} \equiv \mathbf{E}_j^M \mathbf{\Gamma}_j^M, \end{aligned}$$

where $\gamma_j^M = k_{j+1}^M/k_j^M$. It follows that $\|\mathbf{P}_j^M(\mathbf{U}, V_{\text{bias}})\| \leq \|\mathbf{E}_j^M\| \|\mathbf{\Gamma}_j^M\|$. A straightforward computation immediately reveals that

$$(4.1) \quad \|\mathbf{E}_j^M\| \leq e^{L_j^M} |\text{Im } k_j^M| \leq e^{\rho \frac{L}{M}},$$

where $\rho = \sqrt{\frac{2m_0}{\hbar^2} |E - \|\mathbf{U}\|_\infty - |V_{\text{bias}}|}$.

We turn our attention next to estimating $\|\mathbf{\Gamma}_j^M\|$, the spectral norm of the matrix $\mathbf{\Gamma}_j^M$. Once again, an easy computation yields the characteristic equation

$$\det \left((\mathbf{\Gamma}_j^M)^* \mathbf{\Gamma}_j^M - \lambda I \right) = \left(\frac{1 + |\gamma_j^M|^2}{2} - \lambda \right)^2 - \left(\frac{1 - |\gamma_j^M|^2}{2} \right)^2 = 0$$

from which we find the two eigenvalues of $(\mathbf{\Gamma}_j^M)^* \mathbf{\Gamma}_j^M$ to be $\lambda_+^M = 1$ and $\lambda_-^M = |\gamma_j^M|^2$. It follows that

$$\|\mathbf{\Gamma}_j^M\| = \max \left\{ 1, \left| \frac{k_{j+1}^M}{k_j^M} \right| \right\}.$$

Now, for $j \neq 0, M, 2M, 3M, \dots, NM$, from the definition of k_j^M we have that

$$[k_{j+1}^M]^2 = [k_j^M]^2 + \frac{2m_0 V_{\text{bias}} L_j^M}{\hbar^2 L},$$

from which it follows that

$$\left| \frac{k_{j+1}^M}{k_j^M} \right| \leq \left(1 + \frac{2m_0 |V_{\text{bias}}|}{\hbar^2 \delta^2 M} \right)^{\frac{1}{2}}$$

and therefore that

$$(4.2) \quad \|\mathbf{\Gamma}_j^M\| \leq \left(1 + \frac{2m_0 |V_{\text{bias}}|}{\hbar^2 \delta^2 M} \right)^{\frac{1}{2}}.$$

The result then immediately follows from (4.1) and (4.2). \square

LEMMA 4.2. For $j = 0, M, 2M, 3M, \dots, NM$, there exist positive constants ρ and σ which depend on $E, \mathbf{U} = \{U_i\}_{i=1}^N$, and V_{bias} for $V_{\text{min}} \leq V_{\text{bias}} \leq V_{\text{max}}$, but which are independent of j and M such that the bounds

$$\|\mathbf{P}_j^M(\mathbf{U}, V_{\text{bias}})\| \leq \exp(\rho L/M) \sqrt{1 + (2m_0/\hbar^2 \sigma^2) \{2\|\mathbf{U}\|_\infty + |V_{\text{bias}}|\}},$$

$j \neq 0$, and

$$\|\mathbf{P}_0^M(\mathbf{U}, V_{\text{bias}})\| \leq \exp(\rho x_0) \sqrt{1 + (2m_0/\hbar^2 \sigma^2) \{2\|\mathbf{U}\|_\infty + |V_{\text{bias}}|\}}$$

obtain, where for a complex matrix \mathbf{A} , the matrix norm $\|\mathbf{A}\|$ is the spectral norm given by $\|\mathbf{A}\| = \sqrt{\lambda_{\text{max}}(\mathbf{A}^* \mathbf{A})}$.

Proof. For $j = nM, n = 1, 2, \dots, N$, once again from the definition of k_j^M we now have

$$\begin{aligned} [k_{j+1}^M]^2 &= [k_j^M]^2 + \frac{2m_0}{\hbar^2} \left\{ U_n - U_{n+1} + V_{\text{bias}} \left(\frac{x_{nM}^M - x_{nM-1}^M}{L} \right) \right\} \\ &= [k_j^M]^2 + \frac{2m_0}{\hbar^2} \left\{ U_n - U_{n+1} + \frac{V_{\text{bias}} L_{nM}^M}{L} \right\}. \end{aligned}$$

In this case it follows from Assumption 4.1 that

$$\left| \frac{k_{j+1}^M}{k_j^M} \right| \leq \left(1 + \frac{2m_0}{\hbar^2 \delta^2} \left\{ 2 \|\mathbf{U}\|_\infty + \frac{|V_{\text{bias}}|}{M} \right\} \right)^{\frac{1}{2}}$$

and therefore that

$$\|\mathbf{\Gamma}_{nM}^M\| \leq \left(1 + \frac{2m_0}{\hbar^2 \delta^2} \{2 \|\mathbf{U}\|_\infty + |V_{\text{bias}}|\} \right)^{\frac{1}{2}}, \quad n = 1, 2, \dots, N.$$

Finally, for $j = 0$ we obtain

$$\left| \frac{k_1^M}{k_0} \right| \leq \left(1 + \frac{2m_0}{\hbar^2 k_0^2} \{2 \|\mathbf{U}\|_\infty\} \right)^{\frac{1}{2}} \quad \text{and} \quad \|\mathbf{\Gamma}_0^M\| \leq \left(1 + \frac{2m_0}{\hbar^2 k_0^2} \{2 \|\mathbf{U}\|_\infty\} \right)^{\frac{1}{2}}.$$

It remains true that $\|\mathbf{E}_j^M\| \leq e^{L_j^M |Imk_j^M|} \leq e^{\rho \frac{L}{M}}$, $j = M, 2M, 3M, \dots, NM$, and $\|\mathbf{E}_0^M\| \leq e^{x_0 |Imk_0|} \leq e^{\rho x_0}$, and consequently the desired result follows at once. \square

THEOREM 4.3. *The linear discrete dynamical systems given in (3.15) and (3.16) are numerically stable with respect to the approximation index M .*

Proof. Lemmas 4.1 and 4.2 yield

$$\begin{aligned} \left\| \prod_{i=0}^{NM} \mathbf{P}_i^M(\mathbf{U}, V_j) \right\| &\leq \prod_{i=0}^{NM} \|\mathbf{P}_i^M(\mathbf{U}, V_j)\| \\ &= \prod_{i=0}^N \|\mathbf{P}_{iM}^M(\mathbf{U}, V_j)\| \cdot \prod_{\substack{i=1, i \neq nM, \\ n=1, \dots, N-1}}^{NM-1} \|\mathbf{P}_i^M(\mathbf{U}, V_j)\| \\ &\leq e^{\rho x_0} \left(1 + \frac{2m_0}{\hbar^2 \sigma^2} \{2 \|\mathbf{U}\|_\infty + |V_{\text{bias}}|\} \right)^{\frac{1}{2}} \\ &\quad \times \left\{ \prod_{i=1}^N e^{\frac{\rho L}{M}} \left(1 + \frac{2m_0}{\hbar^2 \sigma^2} \{2 \|\mathbf{U}\|_\infty + |V_{\text{bias}}|\} \right)^{\frac{1}{2}} \right\} \\ &\quad \times \left\{ \prod_{\substack{i=1, i \neq nM, \\ n=1, 2, \dots, N-1}}^{NM-1} e^{\frac{\rho L}{M}} \left(1 + \frac{2m_0 |V_{\text{bias}}|}{\hbar^2 \delta^2 M} \right)^{\frac{1}{2}} \right\} \\ &\leq \left(1 + \frac{2m_0}{\hbar^2 \sigma^2} \{2 \|\mathbf{U}\|_\infty + |V_{\text{bias}}|\} \right)^{\frac{N+1}{2}} e^{\rho(x_0 + NL) + \frac{Nm_0 |V_{\text{bias}}|}{\hbar^2 \delta^2}}, \end{aligned}$$

and the result follows. \square

Implicit in our use of the gradient method to solve the approximating optimal design problems was the assumption that the least-squares performance measures J^M given in (3.10) are differentiable with respect to the design parameters $\mathbf{U} = \{U_i\}_{i=1}^N \in \mathbf{R}^N$. It is in fact possible to show that the cost functionals J given by (3.4) and J^M given by (3.10) are differentiable with respect to $\mathbf{U} = \{U_i\}_{i=1}^N \in \mathbf{R}^N$ and, moreover, that $\lim_{M \rightarrow \infty} \nabla J^M(\mathbf{U}^M) = \nabla J(\mathbf{U})$, whenever $\mathbf{U}^M, \mathbf{U} \in \mathbf{R}^N$ with $\lim_{M \rightarrow \infty} \mathbf{U}^M = \mathbf{U}$. It is further possible to establish subsequential convergence of solutions to the approximating finite dimensional optimal design problems defined in section 3 to a solution to the original infinite dimensional optimal design problem.

Toward this end, we reformulate the boundary value problem (3.1)–(3.3) as an abstract elliptic system in weak or variational form. Let H denote the Hilbert space $L_2(x_0, x_N)$ and let $W = H^1(x_0, x_N)$, each endowed with its standard inner product. It follows that W is densely and continuously embedded in H (see, for example, [14]), and then pivoting (see [15], [16], and [17]) on H we obtain the well-known dense and continuous embeddings $W \subset H \subset W^*$, where W^* denotes the space of continuous conjugate linear functionals on W . Let Ω be a compact (i.e., closed and bounded) subset of \mathbf{R}^N , let $|\cdot|_H$, $\|\cdot\|_W$, and $\|\cdot\|_{W^*}$ denote the usual norms on H , W , and W^* , respectively, and let κ denote the continuous embedding constant between H and W , that is, $|\varphi|_H \leq \kappa \|\varphi\|_W$ for $\varphi \in W$.

For each $\mathbf{U} = \{U_i\}_{i=1}^N \in \Omega$, $A_0 \in \mathbf{C}$, and V_{bias} , with $V_{\min} \leq V_{\text{bias}} \leq V_{\max}$, we define the sesquilinear form $a(\mathbf{U}, V_{\text{bias}}; \cdot, \cdot) : W \times W \rightarrow \mathbf{C}$ and the bounded conjugate linear functional $f \in W^*$ by

$$(4.3) \quad \begin{aligned} a(\mathbf{U}, V_{\text{bias}}; \varphi, \chi) &= \int_{x_0}^{x_N} D\varphi(x) D\bar{\chi}(x) dx - \mathbf{i}k_{N+1}\varphi(x_N)\bar{\chi}(x_N) - \mathbf{i}k_0\varphi(x_0)\bar{\chi}(x_0) \\ &+ \frac{2m_0}{\hbar^2} \int_{x_0}^{x_N} \{V(x) - E\} \varphi(x) \bar{\chi}(x) dx, \end{aligned}$$

for $\varphi, \chi \in W$, and by $\langle f, \chi \rangle = -2\mathbf{i}k_0 A_0 e^{\mathbf{i}k_0 x_0} \bar{\chi}(x_0)$, for $\chi \in W$, respectively, where D denotes the differentiation operator with respect to the variable x . The boundary value problem (3.1)–(3.3) is then given in abstract form as finding a $\psi \in W$ that satisfies

$$(4.4) \quad a(\mathbf{U}, V_{\text{bias}}; \psi, \varphi) = \langle f, \varphi \rangle$$

for every $\varphi \in W$.

Straightforward calculations (see, for example, [15]) can be used to establish the following lemma.

LEMMA 4.4. For $\mathbf{U} = \{U_i\}_{i=1}^N \in \Omega$ and V_{bias} with $V_{\min} \leq V_{\text{bias}} \leq V_{\max}$, there exist constants $\lambda \in \mathbf{R}$ and $\alpha, \beta > 0$ which are independent of \mathbf{U} and V_{bias} such that

$$(4.5) \quad |a(\mathbf{U}, V_{\text{bias}}; \varphi, \chi)| \leq \alpha \|\varphi\|_W \|\chi\|_W$$

for $\varphi, \chi \in W$, and

$$(4.6) \quad \operatorname{Re} a(\mathbf{U}, V_{\text{bias}}; \varphi, \varphi) + \lambda |\varphi|_H^2 \geq \beta \|\varphi\|_W^2$$

for every $\varphi \in W$.

Also, there exists a constant $\gamma > 0$ which is independent of V_{bias} such that for every $\mathbf{U}_1 = \{U_i^1\}_{i=1}^N, \mathbf{U}_2 = \{U_i^2\}_{i=1}^N \in \Omega$ we have

$$(4.7) \quad |a(\mathbf{U}_1, V_{\text{bias}}; \varphi, \chi) - a(\mathbf{U}_2, V_{\text{bias}}; \varphi, \chi)| \leq \gamma \|\mathbf{U}_1 - \mathbf{U}_2\|_\infty |\varphi|_H |\chi|_H$$

for $\varphi, \chi \in W$.

In a similar manner, the sequence of approximating discrete two-point boundary value problems given by (3.8) and (3.9) can be reformulated as a sequence of abstract elliptic systems of the form given in (4.4). Indeed, this is achieved by simply replacing the potential function V in (4.3) by the piecewise constant approximation V^M given

by (3.5). Toward this end, for each $M = 1, 2, \dots$, we define the sequence of abstract sesquilinear forms $\{a_M(U, V_{\text{bias}}; \cdot, \cdot)\}_{M=1}^\infty$ on W , $a_M(\mathbf{U}, V_{\text{bias}}; \cdot, \cdot) : W \times W \rightarrow \mathbf{C}$ by

$$(4.8) \quad \begin{aligned} a_M(\mathbf{U}, V_{\text{bias}}; \varphi, \chi) &= \int_{x_0}^{x_N} D\varphi(x) D\bar{\chi}(x) dx - \mathbf{i}k_{N+1}\varphi(x_N)\bar{\chi}(x_N) - \mathbf{i}k_0\varphi(x_0)\bar{\chi}(x_0) \\ &+ \frac{2m_0}{\hbar^2} \int_{x_0}^{x_N} \{V^M(x) - E\} \varphi(x)\bar{\chi}(x) dx, \quad \varphi, \chi \in W, \end{aligned}$$

where the difference between the form defined in (4.3) and the forms defined in (4.8) is that the potential function V given by (2.1) in the form $a(\mathbf{U}, V_{\text{bias}}; \cdot, \cdot) : W \times W \rightarrow \mathbf{C}$ has been replaced by its piecewise constant approximation V^M given in (3.5) by

$$V^M(x) = V\left(x_{(j-1)M+m-1}^M\right), \quad x_{(j-1)M+m-1}^M \leq x < x_{(j-1)M+m}^M,$$

where $j = 1, 2, \dots, N$ and $m = 1, 2, \dots, M$. Once again, it is not difficult to show that the forms $a_M(U, V_{\text{bias}}; \cdot, \cdot) : W \times W \rightarrow \mathbf{C}$ satisfy the inequalities (4.5)–(4.7) with the same constants $\lambda \in \mathbf{R}$ and $\alpha, \beta > 0$ which work for the form $a(\mathbf{U}, V_{\text{bias}}; \cdot, \cdot) : W \times W \rightarrow \mathbf{C}$ given by (4.3).

We consider the sequence of abstract elliptic boundary value problems given by

$$(4.9) \quad a_M(\mathbf{U}, V_{\text{bias}}; \psi^M, \varphi) = \langle f, \varphi \rangle$$

for every $\varphi \in W$.

Under appropriate conditions, a routine application of the Lax–Milgram theorem (see, for example, [15], [16], or [18]) yields the existence of unique solutions to the abstract boundary value problems (4.4) and (4.9). More directly, we have the following well posedness result.

THEOREM 4.5. *If the constant $\lambda \in \mathbf{R}$ and $\beta > 0$ guaranteed to exist by Lemma 4.4 are such that $\lambda < \frac{\beta}{\kappa^2}$, then the abstract elliptic boundary value problem given in (4.4) and the sequence of abstract elliptic boundary value problems given in (4.9) admit unique solutions $\psi \in W$ and $\psi^M \in W$, $M = 1, 2, \dots$.*

Proof. The bound given in (4.5) is sufficient to conclude that the forms a and a^M given in (4.3) and (4.8) define bounded linear operators $A, A_M \in L(W, W^*)$. Moreover, the coercivity estimate given in (4.6) with $\lambda < \frac{\beta}{\kappa^2}$ readily yields the lower bounds $\|A\varphi\|_{W^*} \geq \hat{\beta}\|\varphi\|_W$ and $\|A_M\varphi\|_{W^*} \geq \hat{\beta}\|\varphi\|_W$ with $\hat{\beta} = \beta - \lambda\kappa^2 > 0$. It follows that the mappings A and A_M are injective, and the Riesz representation theorem together with the dense embeddings $W \subset H \subset W^*$ is sufficient to conclude that the mappings are surjective as well. Consequently they each admit bounded inverses A^{-1} and A_M^{-1} with the unique solutions to the boundary value problems (4.4) and (4.9) then given by $\psi = A^{-1}f$ and $\psi_M = A_M^{-1}f$, respectively. We also have the continuous dependence results $\|\psi\|_W \leq \frac{1}{\hat{\beta}}\|f\|_{W^*}$ and $\|\psi_M\|_W \leq \frac{1}{\hat{\beta}}\|f\|_{W^*}$. \square

We note that it is immediately clear that a sufficient condition for $\lambda \leq 0 < \frac{\beta}{\kappa^2}$ would be that the design space Ω , V_{min} , V_{max} and the total energy E are such that there exists a constant $\mu > 0$ such that $\frac{2m_0}{\hbar^2} \{V^M(x) - E\} \geq \mu$ for $x_0 \leq x \leq x_N$.

Recalling the approximation framework developed in section 3, it follows that the functions $\psi^M \in W$ given by

$$\begin{aligned} \psi^M(x) &= \psi^M(x; V_{\text{bias}}, \mathbf{U}) = \psi_{(j-1)M+m}^M(x) \\ &= A_{(j-1)M+m}^M e^{\mathbf{i}k_{(j-1)M+m}^M(x-x_{(j-1)M+m-1}^M)} \\ &+ B_{(j-1)M+m}^M e^{-\mathbf{i}k_{(j-1)M+m}^M(x-x_{(j-1)M+m-1}^M)} \end{aligned}$$

for $x \in [x_{(j-1)M+m-1}^M, x_{(j-1)M+m}^M]$ with coefficients $\{A_{(j-1)M+m}^M\}$ and $\{B_{(j-1)M+m}^M\}$, for $j = 1, 2, \dots, N$ and $m = 1, 2, \dots, M$, determined via the propagation matrix method described in section 3.1 for solving the discrete two-point boundary value problem (3.8), (3.9) above are in fact the unique solutions to the abstract elliptic boundary value problems (4.9) that are guaranteed to exist by Theorem 4.5. Moreover, from (3.7), (3.8), and (3.9) it follows that

$$\begin{aligned} \psi^M(x_N; V_{\text{bias}}, \mathbf{U}) &= \psi_{NM}^M(x_{NM}^M) = A_{NM}^M e^{ik_{NM}^M \frac{L_N}{M}} + B_{NM}^M e^{-ik_{NM}^M \frac{L_N}{M}} \\ &= A_{NM+1}^M + B_{NM+1}^M = A_{NM+1}^M. \end{aligned}$$

Consequently, from (3.10), we find that

$$\begin{aligned} J^M(\mathbf{U}) &= \sum_{j=1}^{\nu} \left| T_0(V_j) - \frac{|A_{NM+1}^M(V_j, \mathbf{U})|^2 k_{N+1,j}}{|A_0|^2 k_0} \right|^2 \\ &= \sum_{j=1}^{\nu} \left| T_0(V_j) - \frac{k_{N+1,j}}{|A_0|^2 k_0} |\psi^M(x_N; V_j, \mathbf{U})|^2 \right|^2 \\ (4.10) \quad &= \sum_{j=1}^{\nu} \left| T_0(V_j) - \frac{k_{N+1,j}}{k_0} |\psi^M(x_N; V_j, \mathbf{U})|^2 \right|^2, \end{aligned}$$

the last expression resulting when A_0 has been arbitrarily set to one.

THEOREM 4.6. *If $\lambda < \frac{\beta}{\kappa^2}$, then for each $M = 1, 2, \dots$, the approximating optimal design problems involving the minimization of the performance indices J^M given in (3.10) (or, equivalently, in (4.10)) over the compact set Ω subject to the boundary value problem given by (3.8), (3.9) (or, equivalently, by (4.9)) have a solution $\hat{\mathbf{U}}^M \in \Omega$.*

Proof. The result will follow immediately if, for each $M = 1, 2, \dots$, we can demonstrate the continuous dependence of $\psi^M(x_N; V_j, \mathbf{U})$ on $\mathbf{U} \in \Omega$. Since $W = H^1(x_0, x_N)$, the Sobolev embedding theorem (see, for example, [7] or [8]) implies that it is sufficient to demonstrate the continuous dependence of $\psi^M(\cdot; V_j, \mathbf{U}) \in W$ on $\mathbf{U} \in \Omega$ with respect to the W -norm. But this result follows immediately from the bounds given in Lemma 4.4. Indeed, for M fixed and $\mathbf{U}, \mathbf{U}_0 \in \Omega$, we let $\psi^M = \psi^M(\cdot; V_j, \mathbf{U}) \in W$ and $\psi_0^M = \psi^M(\cdot; V_j, \mathbf{U}_0) \in W$ denote, respectively, the unique solutions to the abstract elliptic boundary value problem given in (4.9) corresponding to $\mathbf{U} \in \Omega$ and $\mathbf{U}_0 \in \Omega$. Then (4.6), (4.7), and (4.9) yield

$$\begin{aligned} &\beta \|\psi_0^M - \psi^M\|_W^2 \\ &\leq \operatorname{Re} a_M(\mathbf{U}, V_{\text{bias}}; \psi_0^M - \psi^M, \psi_0^M - \psi^M) + \lambda |\psi_0^M - \psi^M|_H^2 \\ &= \operatorname{Re} \{a_M(\mathbf{U}, V_{\text{bias}}; \psi_0^M, \psi_0^M - \psi^M) - a_M(\mathbf{U}, V_{\text{bias}}; \psi^M, \psi_0^M - \psi^M)\} + \lambda |\psi_0^M - \psi^M|_H^2 \\ &= \operatorname{Re} \{a_M(\mathbf{U}, V_{\text{bias}}; \psi_0^M, \psi_0^M - \psi^M) - \langle f, \psi_0^M - \psi^M \rangle\} + \lambda |\psi_0^M - \psi^M|_H^2 \\ &= \operatorname{Re} \{a_M(\mathbf{U}, V_{\text{bias}}; \psi_0^M, \psi_0^M - \psi^M) - a_M(\mathbf{U}_0, V_{\text{bias}}; \psi_0^M, \psi_0^M - \psi^M)\} + \lambda |\psi_0^M - \psi^M|_H^2 \\ &\leq |a_M(\mathbf{U}, V_{\text{bias}}; \psi_0^M, \psi_0^M - \psi^M) - a_M(\mathbf{U}_0, V_{\text{bias}}; \psi_0^M, \psi_0^M - \psi^M)| + \lambda |\psi_0 - \psi^M|_H^2 \\ &\leq \gamma \|\mathbf{U} - \mathbf{U}_0\|_\infty |\psi_0^M|_H |\psi_0^M - \psi^M|_H + \lambda |\psi_0^M - \psi^M|_H^2 \\ &\leq \gamma \kappa \|\mathbf{U} - \mathbf{U}_0\|_\infty |\psi_0^M|_H \|\psi_0^M - \psi^M\|_W + \lambda \kappa^2 \|\psi_0^M - \psi^M\|_W^2. \end{aligned}$$

It then follows that

$$(\beta - \lambda\kappa^2) \|\psi_0^M - \psi^M\|_W^2 \leq \gamma\kappa \|\mathbf{U} - \mathbf{U}_0\|_\infty |\psi_0^M|_H \|\psi_0^M - \psi^M\|_W$$

and therefore that

$$\|\psi_0^M - \psi^M\|_W \leq \frac{\gamma\kappa}{\hat{\beta}} |\psi_0^M|_H \|\mathbf{U}_0 - \mathbf{U}\|_\infty,$$

where $\hat{\beta} = \beta - \lambda\kappa^2 > 0$, and the result follows. \square

Next we establish the existence of the gradients ∇J^M and ∇J of the least-squares performance indices J^M given in (3.10) and J given in (3.4).

THEOREM 4.7. *If $\lambda < \frac{\beta}{\kappa^2}$, then the approximating optimal design performance indices J^M , for each $M = 1, 2, \dots$, given in (3.10) (or, equivalently, (4.10)) and the performance index J given in (3.4) are differentiable with respect to $\mathbf{U} = \{U_i\}_{i=1}^N \in \text{int}(\Omega)$.*

Proof. We demonstrate the differentiability of J . Establishing the differentiability of J^M is completely analogous. Also, it is immediately clear that in order to establish that J is differentiable, it suffices to show that the unique solution $\psi \in W$ to the abstract boundary value problem (4.4) guaranteed to exist by Theorem 4.5 is differentiable with respect to $\mathbf{U} = \{U_i\}_{i=1}^N \in \text{int}(\Omega)$.

Let $\psi_0 \in W$ denote the unique solution to (4.4), and, for $h > 0$ sufficiently small, let $\psi_j \in W$ be the unique solution to the abstract boundary value problem

$$a(\mathbf{U} + h\mathbf{e}_j, V_{\text{bias}}; \psi_j, \varphi) = \langle f, \varphi \rangle \quad \text{for every } \varphi \in W,$$

where $\mathbf{e}_j \in \mathbf{R}^N$, $j = 1, 2, \dots, N$, denote the standard basis elements in \mathbf{R}^N . In addition, for $j = 1, 2, \dots, N$ and $\psi \in W$, let $\ell_{\psi,j} \in W^*$ be given by

$$\ell_{\psi,j}(\varphi) = -\frac{2m_0}{h^2} \int_{x_0}^{x_N} \chi_{[x_{j-1}, x_j]}(x) \psi(x) \bar{\varphi}(x) dx \quad \text{for every } \varphi \in W,$$

where χ_I denotes the characteristic function of the interval $I \subseteq \mathbf{R}$, and let $\psi'_j \in W$ be the unique solution to the abstract boundary value problem

$$(4.11) \quad a(\mathbf{U}, V_{\text{bias}}; \psi'_j, \varphi) = \ell_{\psi_0,j}(\varphi)$$

for every $\varphi \in W$, also guaranteed to exist by Theorem 4.5. Then, setting $\psi_{j,h} = \psi'_j - \frac{\psi_j - \psi_0}{h}$, for $j = 1, 2, \dots, N$, the $W - H$ coercivity inequality (4.6) yields

$$\beta \|\psi_{j,h}\|_W^2 \leq \text{Re } a(\mathbf{U}, V_{\text{bias}}; \psi_{j,h}, \psi_{j,h}) + \lambda |\psi_{j,h}|_H^2.$$

Once again, setting $\hat{\beta} = \beta - \lambda\kappa^2 > 0$, it follows that

$$\begin{aligned} \hat{\beta} \|\psi_{j,h}\|_W^2 &\leq \text{Re } a(\mathbf{U}, V_{\text{bias}}; \psi_{j,h}, \psi_{j,h}) \\ &= \text{Re} \left\{ \ell_{\psi_0,j}(\psi_{j,h}) + \frac{1}{h} a(\mathbf{U}, V_{\text{bias}}; \psi_0, \psi_{j,h}) - \frac{1}{h} a(\mathbf{U}, V_{\text{bias}}; \psi_j, \psi_{j,h}) \right\} \\ &= \text{Re} \left\{ \ell_{\psi_0,j}(\psi_{j,h}) + \frac{1}{h} a(\mathbf{U} + h\mathbf{e}_j, V_{\text{bias}}; \psi_j, \psi_{j,h}) - \frac{1}{h} a(\mathbf{U}, V_{\text{bias}}; \psi_j, \psi_{j,h}) \right\} \\ &= \text{Re} \left\{ \ell_{\psi_0,j}(\psi_{j,h}) - \ell_{\psi_j,j}(\psi_{j,h}) \right\}. \end{aligned}$$

It follows that

$$\|\psi_{j,h}\|_W \leq \frac{2m_0\kappa^2}{\hat{\beta}\hbar^2} \|\psi_j - \psi_0\|_W.$$

A similar straightforward calculation yields

$$\begin{aligned} \hat{\beta} \|\psi_j - \psi_0\|_W^2 &\leq \operatorname{Re} a(\mathbf{U} + h\mathbf{e}_j, V_{\text{bias}}; \psi_j - \psi_0, \psi_j - \psi_0) \\ &= \operatorname{Re} \left\{ -\frac{2m_0h}{\hbar^2} \int_{x_0}^{x_N} \chi_{[x_{j-1}, x_j]} \psi_0 (\bar{\psi}_j - \bar{\psi}_0) dx \right\} \\ &= \frac{2m_0\kappa^2 h}{\hbar^2} \|\psi_0\|_W \|\psi_j - \psi_0\|_W, \end{aligned}$$

and, consequently, that

$$\|\psi_j - \psi_0\|_W \leq \frac{2m_0\kappa^2}{\hat{\beta}\hbar^2} \|\psi_0\|_W h.$$

Combining our two estimates, we obtain

$$\left\| \psi'_j - \frac{\psi_j - \psi_0}{h} \right\|_W \leq \frac{4m_0^2\kappa^4}{\hat{\beta}\hbar^4} \|\psi_0\|_W h$$

from which the desired result immediately follows with $\nabla_U \psi_0 = [\psi'_1, \psi'_2, \dots, \psi'_N] \in \times_{j=1}^N W$. \square

We conclude this section with the following two convergence results. The first is concerned with the subsequential convergence of the solutions of the approximating optimal design problems $\hat{\mathbf{U}}^M \in \Omega$ to a solution $\hat{\mathbf{U}} \in \Omega$ of the original optimal design problem. The second involves the convergence of the gradients of the approximating cost functionals ∇J^M to the gradient of the original cost functional ∇J .

THEOREM 4.8. *Let $\lambda < \frac{\beta}{\kappa^2}$, and, for each $M = 1, 2, \dots$, let $\hat{\mathbf{U}}^M \in \Omega$ be the solution to the M th approximating optimal design problem. Then the sequence $\{\hat{\mathbf{U}}^M\}_{M=1}^\infty \subset \Omega$ admits a convergent subsequence $\{\hat{\mathbf{U}}^{M_k}\}_{k=1}^\infty \subset \{\hat{\mathbf{U}}^M\}_{M=1}^\infty \subset \Omega$ with $\lim_{k \rightarrow \infty} \hat{\mathbf{U}}^{M_k} = \hat{\mathbf{U}} \in \Omega$. Moreover, $\hat{\mathbf{U}} \in \Omega$ is a solution to the optimal design problem given by (3.1)–(3.4) in the sense that $J(\hat{\mathbf{U}}) = \min_{\mathbf{U} \in \Omega} J(\mathbf{U})$.*

Proof. The existence of the convergent subsequence $\{\hat{\mathbf{U}}^{M_k}\}_{k=1}^\infty \subset \{\hat{\mathbf{U}}^M\}_{M=1}^\infty \subset \Omega$ with $\lim_{k \rightarrow \infty} \hat{\mathbf{U}}^{M_k} = \hat{\mathbf{U}} \in \Omega$ follows immediately from the assumption that Ω is a closed and bounded (and therefore compact) subset of \mathbf{R}^N . Now let $\{\mathbf{U}^M\}_{M=1}^\infty \subset \Omega$ be any convergent sequence in Ω with $\lim_{M \rightarrow \infty} \mathbf{U}^M = \mathbf{U}_0 \in \Omega$, and, for each $M = 1, 2, \dots$, let ψ^M denote the unique solution to the abstract elliptic boundary value problem given in (4.9) with $\mathbf{U} = \mathbf{U}^M$ and let ψ_0 denote the unique solution to the abstract elliptic boundary value problem given in (4.4) with $\mathbf{U} = \mathbf{U}_0$. Then, the bounds given in Lemma 4.4 imply

$$\begin{aligned} \beta \|\psi_0 - \psi^M\|_W^2 &\leq \operatorname{Re} a_M(\mathbf{U}^M, V_{\text{bias}}; \psi_0 - \psi^M, \psi_0 - \psi^M) + \lambda |\psi_0 - \psi^M|_H^2 \\ &= \operatorname{Re} \left\{ a_M(\mathbf{U}^M, V_{\text{bias}}; \psi_0, \psi_0 - \psi^M) - a_M(\mathbf{U}^M, V_{\text{bias}}; \psi^M, \psi_0 - \psi^M) \right\} \\ &\quad + \lambda |\psi_0 - \psi^M|_H^2 \end{aligned}$$

$$\begin{aligned}
 &= \operatorname{Re} \left\{ a_M \left(\mathbf{U}^M, V_{\text{bias}}; \psi_0, \psi_0 - \psi^M \right) - \langle f, \psi_0 - \psi^M \rangle \right\} + \lambda |\psi_0 - \psi^M|_H^2 \\
 &= \operatorname{Re} \left\{ a_M \left(\mathbf{U}^M, V_{\text{bias}}; \psi_0, \psi_0 - \psi^M \right) - a \left(\mathbf{U}_0, V_{\text{bias}}; \psi_0, \psi_0 - \psi^M \right) \right\} + \lambda |\psi_0 - \psi^M|_H^2 \\
 &= \operatorname{Re} \left\{ a_M \left(\mathbf{U}^M, V_{\text{bias}}; \psi_0, \psi_0 - \psi^M \right) - a_M \left(\mathbf{U}_0, V_{\text{bias}}; \psi_0, \psi_0 - \psi^M \right) \right\} \\
 &\quad + \operatorname{Re} \left\{ a_M \left(\mathbf{U}_0, V_{\text{bias}}; \psi_0, \psi_0 - \psi^M \right) - a \left(\mathbf{U}_0, V_{\text{bias}}; \psi_0, \psi_0 - \psi^M \right) \right\} + \lambda |\psi_0 - \psi^M|_H^2 \\
 &\leq \gamma \kappa \left\| \mathbf{U}^M - \mathbf{U}_0 \right\|_\infty |\psi_0|_H \|\psi_0 - \psi^M\|_W \\
 &\quad + \frac{2m_0}{\hbar^2} \int_{x_0}^{x_N} \{V^M(x) - V(x)\} \psi_0(x) (\bar{\psi}_0(x) - \bar{\psi}^M(x)) dx + \lambda \kappa^2 \|\psi_0 - \psi^M\|_W^2 \\
 &\leq \gamma \kappa \left\| \mathbf{U}^M - \mathbf{U}_0 \right\|_\infty |\psi_0|_H \|\psi_0 - \psi^M\|_W \\
 &\quad + \frac{2m_0 |V_{\text{bias}}|}{\hbar^2} \sum_{j=1}^N \int_{x_{j-1}}^{x_j} \frac{L_j}{ML} |\psi_0(x)| |\bar{\psi}_0(x) - \bar{\psi}^M(x)| dx + \lambda \kappa^2 \|\psi_0 - \psi^M\|_W^2 \\
 &\leq \gamma \kappa \left\| \mathbf{U}^M - \mathbf{U}_0 \right\|_\infty |\psi_0|_H \|\psi_0 - \psi^M\|_W + \frac{2m_0 \kappa |V_{\text{bias}}|}{\hbar^2 M} |\psi_0|_H \|\psi_0 - \psi^M\|_W \\
 &\quad + \lambda \kappa^2 \|\psi_0 - \psi^M\|_W^2.
 \end{aligned}$$

It then follows that

$$\begin{aligned}
 (\beta - \lambda \kappa^2) \|\psi_0 - \psi^M\|_W^2 &\leq \gamma \kappa \left\| \mathbf{U}^M - \mathbf{U}_0 \right\|_\infty |\psi_0|_H \|\psi_0 - \psi^M\|_W \\
 &\quad + \frac{2m_0 \kappa |V_{\text{bias}}|}{\hbar^2 M} |\psi_0|_H \|\psi_0 - \psi^M\|_W
 \end{aligned}$$

and therefore that

$$(4.12) \quad \|\psi_0 - \psi^M\|_W \leq \frac{\gamma \kappa}{\hat{\beta}} \left\| \mathbf{U}^M - \mathbf{U}_0 \right\|_\infty |\psi_0|_H + \frac{2m_0 \kappa |V_{\text{bias}}|}{\hat{\beta} \hbar^2 M} |\psi_0|_H,$$

where once again $\hat{\beta} = \beta - \lambda \kappa^2 > 0$. Consequently, we have

$$\lim_{M \rightarrow \infty} \psi^M \left(\cdot; V_{\text{bias}}, \mathbf{U}^M \right) = \psi_0 \left(\cdot; V_{\text{bias}}, \mathbf{U}_0 \right)$$

in W and, once again by the Sobolev embedding theorem [14], in $C[x_0, x_N]$ as well. Finally, for any $\mathbf{U} \in \Omega$ we find that

$$J \left(\hat{\mathbf{U}} \right) = J \left(\lim_{k \rightarrow \infty} \hat{\mathbf{U}}^{M_k} \right) = \lim_{k \rightarrow \infty} J^{M_k} \left(\hat{\mathbf{U}}^{M_k} \right) \leq \lim_{k \rightarrow \infty} J^{M_k} \left(\mathbf{U} \right) = J \left(\mathbf{U} \right),$$

and the desired result has been established. \square

THEOREM 4.9. *Let $\lambda < \frac{\beta}{\kappa^2}$, and, for each $M = 1, 2, \dots$, let $\mathbf{U}^M \in \Omega$ with $\lim_{k \rightarrow \infty} \mathbf{U}^M = \mathbf{U}_0 \in \Omega$. Then $\nabla J \left(\mathbf{U}_0 \right) = \lim_{M \rightarrow \infty} \nabla J^M \left(\mathbf{U}^M \right)$.*

Proof. For each $M = 1, 2, \dots$ let $\psi^M \in W$ denote the unique solution to the abstract boundary value problem given in (4.9) with $\mathbf{U} = \mathbf{U}^M$, and let $\psi_0 \in W$ denote the unique solution to the abstract boundary value problem given in (4.4) with $\mathbf{U} = \mathbf{U}_0$. Then from Theorem 4.7 we know that, for each $j = 1, 2, \dots, N$, there exists $\psi'_j \in W$ with $\nabla_{\mathbf{U}} \psi_0 = [\psi'_1, \psi'_2, \dots, \psi'_N] \in \times_{j=1}^N W$ and that, for each $M = 1, 2, \dots$ and each $j = 1, 2, \dots, N$, there exists $\psi'^M_j \in W$ such that $\nabla_{\mathbf{U}} \psi^M = [\psi'^M_1, \psi'^M_2, \dots, \psi'^M_N] \in$

$\times_{j=1}^N W$. We show that, for each $j = 1, 2, \dots, N$, $\lim_{M \rightarrow \infty} \psi_j^{\prime M} = \psi_j'$ in W , and hence that $\lim_{M \rightarrow \infty} \nabla_{\mathbf{U}} \psi^M = \nabla_{\mathbf{U}} \psi_0$ in $\times_{j=1}^N W$. Then the desired result will immediately follow from the Sobolev embedding theorem [14]. For each $j = 1, 2, \dots, N$, the coercivity inequality (4.6), the fact that $\lambda < \frac{\beta}{\kappa^2}$, the definition (4.11), and estimates similar to those in the proof of Theorem 4.8 yield

$$\begin{aligned} \hat{\beta} \left\| \psi_j' - \psi_j^{\prime M} \right\|_W^2 &\leq \operatorname{Re} \left\{ a_M \left(\mathbf{U}^M, V_{\text{bias}}; \psi_j' - \psi_j^{\prime M}, \psi_j' - \psi_j^{\prime M} \right) \right\} \\ &= \operatorname{Re} \left\{ a_M \left(\mathbf{U}^M, V_{\text{bias}}; \psi_j', \psi_j' - \psi_j^{\prime M} \right) - a_M \left(\mathbf{U}_0, V_{\text{bias}}; \psi_j', \psi_j' - \psi_j^{\prime M} \right) \right. \\ &\quad \left. + a_M \left(\mathbf{U}_0, V_{\text{bias}}; \psi_j', \psi_j' - \psi_j^{\prime M} \right) - a \left(\mathbf{U}_0, V_{\text{bias}}; \psi_j', \psi_j' - \psi_j^{\prime M} \right) \right. \\ &= a \left(\mathbf{U}^M, V_{\text{bias}}; \psi_j', \psi_j' - \psi_j^{\prime M} \right) + a \left(\mathbf{U}_0, V_{\text{bias}}; \psi_j', \psi_j' - \psi_j^{\prime M} \right) \\ &\quad \left. - a_M \left(\mathbf{U}^M, V_{\text{bias}}; \psi_j^{\prime M}, \psi_j' - \psi_j^{\prime M} \right) \right\} \\ &\leq \gamma \kappa^2 \left\| \mathbf{U}^M - \mathbf{U}_0 \right\|_{\infty} \left\| \psi_j' \right\|_W \left\| \psi_j' - \psi_j^{\prime M} \right\|_W \\ &\quad + \frac{2m_0}{\hbar^2} \int_{x_0}^{x_N} |V^M(x) - V(x)| |\psi_j'(x)| |\psi_j'(x) - \psi_j^{\prime M}(x)| dx \\ &\quad + \left| \ell_{\psi_0^M, j}(\psi_j' - \psi_j^{\prime M}) - \ell_{\psi_0, j}(\psi_j' - \psi_j^{\prime M}) \right| \\ &\leq \gamma \kappa^2 \left\| \mathbf{U}^M - \mathbf{U}_0 \right\|_{\infty} \left\| \psi_j' \right\|_W \left\| \psi_j' - \psi_j^{\prime M} \right\|_W + \frac{2m_0 \kappa^2 |V_{\text{bias}}|}{\hbar^2 M} \left\| \psi_j' \right\|_W \left\| \psi_j' - \psi_j^{\prime M} \right\|_W \\ &\quad + \frac{2m_0 \kappa^2}{\hbar^2} \left\| \psi^M - \psi_0 \right\|_W \left\| \psi_j' - \psi_j^{\prime M} \right\|_W, \end{aligned}$$

where once again $\hat{\beta} = \beta - \lambda \kappa^2 > 0$. It then follows that

$$\begin{aligned} \left\| \psi_j' - \psi_j^{\prime M} \right\|_W &\leq \frac{\gamma \kappa^2}{\hat{\beta}} \left\| \psi_j' \right\|_W \left\| \mathbf{U}^M - \mathbf{U}_0 \right\|_{\infty} + \frac{2m_0 \kappa^2 |V_{\text{bias}}|}{\hat{\beta} \hbar^2 M} \left\| \psi_j' \right\|_W \\ &\quad + \frac{2m_0 \kappa^2}{\hat{\beta} \hbar^2} \left\| \psi^M - \psi_0 \right\|_W, \end{aligned}$$

and, therefore, making use of the estimate given in (4.12), that

$$(4.13) \quad \begin{aligned} \left\| \psi_j' - \psi_j^{\prime M} \right\|_W &\leq \left\{ \frac{\gamma \kappa^2}{\hat{\beta}} \left\| \psi_j' \right\|_W + \frac{2m_0 \kappa^4}{\hat{\beta}^2 \hbar^2} \left\| \psi_0 \right\|_W \right\} \left\| \mathbf{U}^M - \mathbf{U}_0 \right\|_{\infty} \\ &\quad + \left\{ \frac{2m_0 \kappa^2 |V_{\text{bias}}|}{\hat{\beta} \hbar^2} \left\| \psi_j' \right\|_W + \frac{4m_0^2 \kappa^4 |V_{\text{bias}}|}{\hat{\beta}^2 \hbar^4} \left\| \psi_0 \right\|_W \right\} \frac{1}{M}, \end{aligned}$$

from which the desired result then immediately follows. \square

It is in fact also possible to characterize both the gradient of J and the gradient of J^M and the convergence of ∇J^M to ∇J as $M \rightarrow \infty$ through the use of an adjoint and a costate variable. Indeed, for each $\mathbf{U}_0 \in \Omega$, $j = 1, 2, \dots, \nu$, a straightforward calculation yields the adjoint and gradient formula

$$a(\mathbf{U}_0, V_j; \psi_j, \varphi) = \langle f, \varphi \rangle \quad \text{for every } \varphi \in W,$$

$$\overline{a(\mathbf{U}_0, V_j; \varphi, \eta_j)} = \langle g_j(\psi_j), \varphi \rangle \quad \text{for every } \varphi \in W,$$

(4.14)

$$\begin{aligned} & \nabla J(\mathbf{U}) \\ &= \frac{2m_0}{\hbar^2} \operatorname{Re} \sum_{j=1}^{\nu} \left[\int_{x_0}^{x_1} \psi_j(x) \overline{\eta_j(x)} dx, \int_{x_1}^{x_2} \psi_j(x) \overline{\eta_j(x)} dx, \dots, \int_{x_{N-1}}^{x_N} \psi_j(x) \overline{\eta_j(x)} dx \right], \end{aligned}$$

where, for $\varphi, \psi \in W$, $g_j(\psi) \in W^*$ is given by

$$\langle g_j(\psi), \varphi \rangle = -\frac{4k_{N+1,j}}{k_0} \left[T_0(V_j) - \frac{k_{N+1,j}}{k_0} |\psi_j(x_N)|^2 \right] \psi_j(x_N) \overline{\varphi(x_N)}.$$

Similarly, for each $j = 1, 2, \dots, \nu$, each $M = 1, 2, \dots$, and $\mathbf{U}^M \in \Omega$, we have

$$a_M(\mathbf{U}^M, V_j; \psi_j^M, \varphi) = \langle f, \varphi \rangle \quad \text{for every } \varphi \in W,$$

$$\overline{a_M(\mathbf{U}^M, V_j; \varphi, \eta_j^M)} = \langle g_j(\psi_j^M), \varphi \rangle \quad \text{for every } \varphi \in W,$$

(4.15)

$$\begin{aligned} & \nabla J^M(\mathbf{U}) \\ &= \frac{2m_0}{\hbar^2} \operatorname{Re} \sum_{j=1}^{\nu} \left[\int_{x_0}^{x_1} \psi_j^M(x) \overline{\eta_j^M(x)} dx, \int_{x_1}^{x_2} \psi_j^M(x) \overline{\eta_j^M(x)} dx, \dots, \int_{x_{N-1}}^{x_N} \psi_j^M(x) \overline{\eta_j^M(x)} dx \right]. \end{aligned}$$

Then if $\lambda < \frac{\beta}{\kappa^2}$ and $\lim_{M \rightarrow \infty} \mathbf{U}^M = \mathbf{U}_0 \in \Omega$, as in the proof of Theorem 4.8, for each $j = 1, 2, \dots, \nu$, we have $\lim_{M \rightarrow \infty} \psi_j^M = \psi_j$ in W , from which it is straightforward to show $\lim_{M \rightarrow \infty} g_j(\psi_j^M) = g_j(\psi)$ in W^* or, equivalently, that $\lim_{M \rightarrow \infty} \|g_j(\psi_j^M) - g_j(\psi)\|_{W^*} = 0$. A coercivity argument analogous to those used in the proofs of the theorems above can then be used to argue costate convergence. That is, we have that $\lim_{M \rightarrow \infty} \eta_j^M = \eta_j$ in W . The convergence of the gradients given by $\lim_{M \rightarrow \infty} \nabla J^M(\mathbf{U}_M) = \nabla J(\mathbf{U}_0) \in \mathbf{R}^N$ then follows immediately from (4.14), (4.15), the continuity of the H inner product, and the continuous embedding of W in H .

5. Numerical studies. In this section we present the results of some of our numerical studies involving the approach discussed above. In particular, we consider the optimal design of three different 10-layer devices in each of which all of the layers have the same thickness of 1 nm. One device is to have a linear transmission function T_{01} , a second is to have a quadratic transmission function T_{02} , and the third is to have a square root transmission function T_{03} . More precisely, we take

$$(5.1) \quad T_{01}(V) = 0.1V + 0.005,$$

$$(5.2) \quad T_{02}(V) = 0.05V^2 + 0.015V + 0.001,$$

and

$$(5.3) \quad T_{03}(V) = 0.05\sqrt{V} + 0.005.$$

We base our design on 26 equally spaced bias voltages from $V_{\min} = 0$ V to $V_{\max} = 0.25$ V. It follows that we set $N = 10$; $L = 10$; $x_i = i$, $i = 0, 1, 2, \dots, N$; $L_i = 1$,

$i = 1, 2, \dots, N$; $\nu = 26$; $V_{\min} = 0$; $V_{\max} = 0.25$; and $V_j = V_{\min} + j \frac{V_{\max} - V_{\min}}{\nu}$, $j = 0, 1, 2, \dots, \nu$.

All computations were carried out on a PC using MATLAB. The resulting approximating optimization problems were solved using the MATLAB constrained optimization routine FMINCON. The requisite gradients were computed via the adjoint-based method described in section 3.2. An initial guess for the layer potential energies had to be supplied. We took it to be constant across all the layers of the device at 0.5 eV. The feasible potential energy levels were constrained to remain between $U_L = 0$ eV and $U_H = 1$ eV. In our calculations we set the incident electron energy to be $E = 0.026$ eV and the effective electron mass $m^* = 0.07 \times m_0$, where $m_0 = 9.10939 \times 10^{-31}$ kg is the bare electron mass. This choice of m^* is appropriate for an electron in the conduction band of $\text{Al}_\xi \text{Ga}_{1-\xi} \text{As}$.

We determined optimal designs with discretization levels $M = 2, 4, 8, 16, 32, 64, 128$. To evaluate the performance of our scheme we simulated the performance of the optimal designs by evaluating the least-squares performance index (3.4), using the propagation matrix method to solve the Schrödinger equation discretized at the level of $M = 512$. To attempt to observe the convergence of the optimal designs, we computed the relative error between the optimal design for discretization level M and the optimal design for discretization level $M = 128$ in both the L_2 - and L_∞ -norms. Finally we also recorded the number of FMINCON iterations that were required until convergence was achieved and calculated the number of CPU seconds per iteration. For each of the desired transmission coefficients given in (5.1)–(5.3), we tabulated our results in Tables 5.1–5.3. In Figures 5.1–5.6 we plot the potential energy profiles and the values of the transmission function at the bias voltage levels $V_j = V_{\min} + j \frac{V_{\max} - V_{\min}}{\nu}$, $j = 0, 1, 2, \dots, \nu$, for each of the optimal designs for each of the three desired characteristics given in equations (5.1)–(5.3). Once again, to simulate the actual performance of the optimal designs, in calculating the transmission functions we discretized the Schrödinger equation using the approach we have described here at discretization level $M = 512$.

TABLE 5.1

Tabulated results for the optimal potential energy profiles for Device 1 given by (5.1) for different discretization levels.

| M | $J^M(\hat{\mathbf{U}}^M)$ | $J^{512}(\hat{\mathbf{U}}^M)$ | $\frac{\ \hat{\mathbf{U}}^M - \hat{\mathbf{U}}^{128}\ _2}{\ \hat{\mathbf{U}}^{128}\ _2}$ | $\frac{\ \hat{\mathbf{U}}^M - \hat{\mathbf{U}}^{128}\ _\infty}{\ \hat{\mathbf{U}}^{128}\ _\infty}$ | Iter | CPU/iter (sec/iter) |
|-----|---------------------------|-------------------------------|--|--|------|------------------------|
| 2 | 1.73×10^{-8} | 9.96×10^{-5} | 0.09 | 0.12 | 204 | 1.40 |
| 4 | 1.71×10^{-8} | 2.22×10^{-5} | 0.11 | 0.10 | 32 | 2.62 |
| 8 | 1.31×10^{-8} | 0.51×10^{-5} | 0.12 | 0.18 | 41 | 5.47 |
| 16 | 1.68×10^{-8} | 0.12×10^{-5} | 0.08 | 0.10 | 46 | 10.72 |
| 32 | 1.63×10^{-8} | 0.03×10^{-5} | 0.08 | 0.09 | 63 | 9.50 |
| 64 | 1.65×10^{-8} | 0.01×10^{-5} | 0.01 | 0.02 | 63 | 45.97 |
| 128 | 1.80×10^{-8} | 0.00×10^{-5} | 0.00 | 0.00 | 59 | 95.82 |

Inspection of the tables reveals (and not surprisingly) that performance improves with increasing level of discretization. Also, for each device, although the locally optimal designs we find are clustered, and some degree of convergence is observed, it is by no means monotone.

Finally, we numerically illustrate the gradient convergence result given in Theorem 4.9. Once again with $N = 10$; $L = 10$; $x_i = i$, $i = 0, 1, 2, \dots, N$; $L_i = 1$, $i = 1, 2, \dots, N$; $\nu = 26$; $V_{\min} = 0$; $V_{\max} = 0.25$; $V_j = V_{\min} + j \frac{V_{\max} - V_{\min}}{\nu}$ for

TABLE 5.2

Tabulated results for the optimal potential energy profiles for Device 2 given by (5.2) for different discretization levels.

| M | $J^M(\hat{\mathbf{U}}^M)$ | $J^{512}(\hat{\mathbf{U}}^M)$ | $\frac{\ \hat{\mathbf{U}}^M - \hat{\mathbf{U}}^{128}\ _2}{\ \hat{\mathbf{U}}^{128}\ _2}$ | $\frac{\ \hat{\mathbf{U}}^M - \hat{\mathbf{U}}^{128}\ _\infty}{\ \hat{\mathbf{U}}^{128}\ _\infty}$ | Iter | CPU/iter (sec/iter) |
|-----|---------------------------|-------------------------------|--|--|------|------------------------|
| 2 | 1.06×10^{-8} | 7.11×10^{-6} | 0.22 | 0.30 | 26 | 1.67 |
| 4 | 1.13×10^{-8} | 1.50×10^{-6} | 0.12 | 0.13 | 38 | 3.02 |
| 8 | 0.56×10^{-8} | 0.35×10^{-6} | 0.04 | 0.05 | 24 | 5.92 |
| 16 | 1.85×10^{-8} | 0.11×10^{-6} | 0.15 | 0.17 | 38 | 10.57 |
| 32 | 1.20×10^{-8} | 0.03×10^{-6} | 0.06 | 0.06 | 34 | 21.85 |
| 64 | 0.51×10^{-8} | 0.01×10^{-6} | 0.09 | 0.10 | 55 | 44.25 |
| 128 | 1.03×10^{-8} | 0.01×10^{-6} | 0.00 | 0.00 | 107 | 99.24 |

TABLE 5.3

Tabulated results for the optimal potential energy profiles for Device 3 given by (5.3) for different discretization levels.

| M | $J^M(\hat{\mathbf{U}}^M)$ | $J^{512}(\hat{\mathbf{U}}^M)$ | $\frac{\ \hat{\mathbf{U}} - \hat{\mathbf{U}}^{128}\ _2}{\ \hat{\mathbf{U}}^{128}\ _2}$ | $\frac{\ \hat{\mathbf{U}}^M - \hat{\mathbf{U}}^{128}\ _\infty}{\ \hat{\mathbf{U}}^{128}\ _\infty}$ | Iter | CPU/iter (sec/iter) |
|-----|---------------------------|-------------------------------|--|--|------|------------------------|
| 2 | 0.97×10^{-5} | 8.85×10^{-5} | 0.21 | 0.19 | 61 | 1.59 |
| 4 | 0.94×10^{-5} | 2.67×10^{-5} | 0.11 | 0.09 | 92 | 3.12 |
| 8 | 1.33×10^{-5} | 1.32×10^{-5} | 0.09 | 0.10 | 125 | 5.49 |
| 16 | 0.92×10^{-5} | 1.01×10^{-5} | 0.08 | 0.07 | 400 | 10.47 |
| 32 | 0.92×10^{-5} | 0.94×10^{-5} | 0.05 | 0.06 | 96 | 21.81 |
| 64 | 0.92×10^{-5} | 0.92×10^{-5} | 0.06 | 0.05 | 123 | 44.69 |
| 128 | 0.91×10^{-5} | 0.91×10^{-5} | 0.00 | 0.00 | 173 | 95.65 |

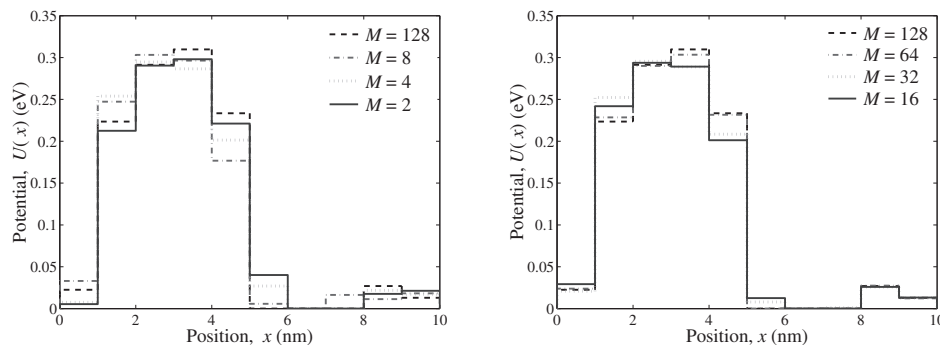


FIG. 5.1. Optimal potential energy profiles for Device 1 given by (5.1) for discretization levels $M = 2, 4, 8, 128$ (left) and $M = 16, 32, 64, 128$ (right).

$j = 0, 1, 2, \dots, \nu$; transmission function $T_0(V) = T_{02}(V)$ given in (5.2) (i.e., Device 2); and $\mathbf{U} = \{U_i\}_{i=1}^N \in \mathbf{R}^N$ randomly generated, we used the adjoint-based scheme described in section 3 to compute $\nabla J^M(\mathbf{U}) \in \mathbf{R}^N$ for $M = 2, 4, 8, \dots, 2048$. To illustrate convergence, in Table 5.4 we tabulated $\frac{\|\nabla J^M(\mathbf{U}) - \nabla J^{2048}(\mathbf{U})\|_2}{\|\nabla J^{2048}(\mathbf{U})\|_2}$ for $M = 4, 8, \dots, 1024$. The linear convergence predicted by the estimates (4.12) in the proof of Theorem 4.8 and (4.13) in the proof of Theorem 4.9 is immediately evident in the table.

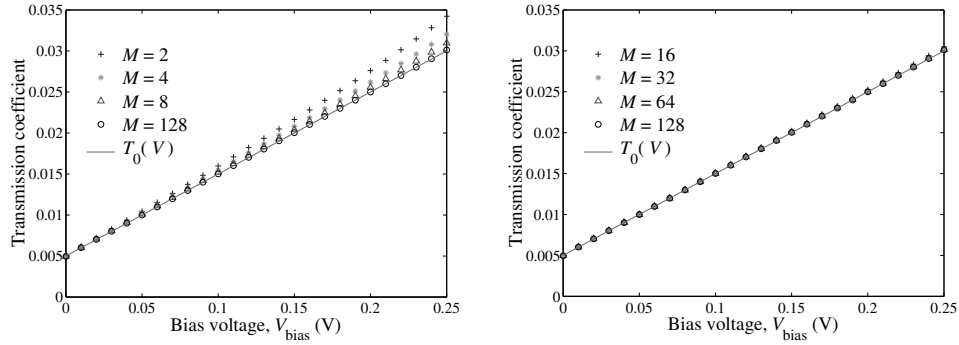


FIG. 5.2. Simulated value of transmission function at bias voltage design values using optimal potential energy profiles for Device 1 given by (5.1) for discretization levels $M = 2, 4, 8, 128$ (left) and $M = 16, 32, 64, 128$ (right).

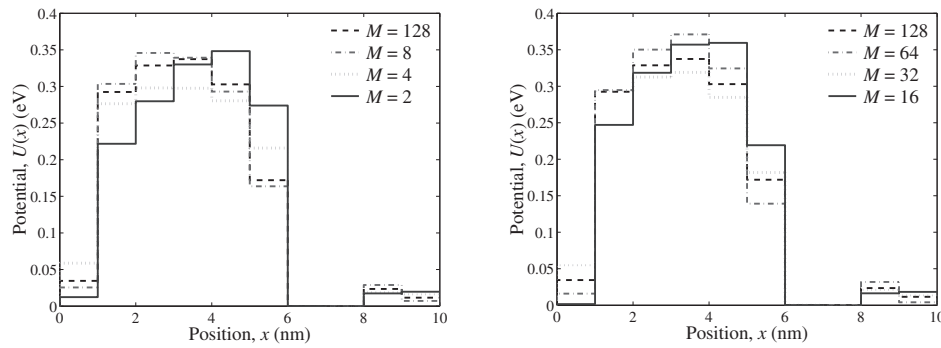


FIG. 5.3. Optimal potential energy profiles for Device 2 given by (5.2) for discretization levels $M = 2, 4, 8, 128$ (left) and $M = 16, 32, 64, 128$ (right).

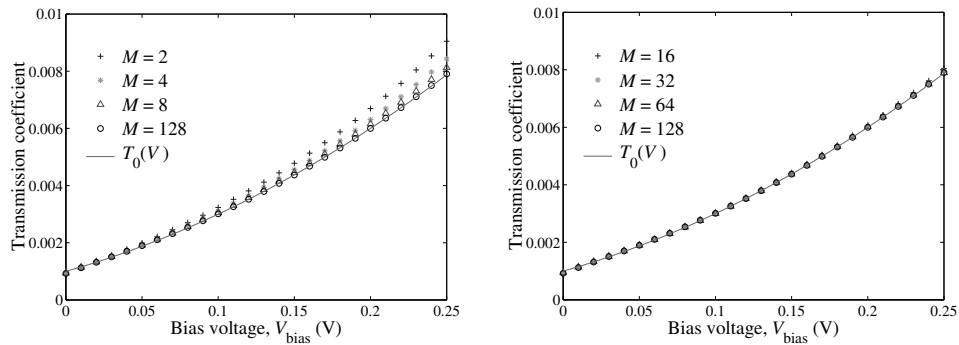


FIG. 5.4. Simulated value of transmission function at bias voltage design values using optimal potential energy profiles for Device 2 given by (5.2) for discretization levels $M = 2, 4, 8, 128$ (left) and $M = 16, 32, 64, 128$ (right).

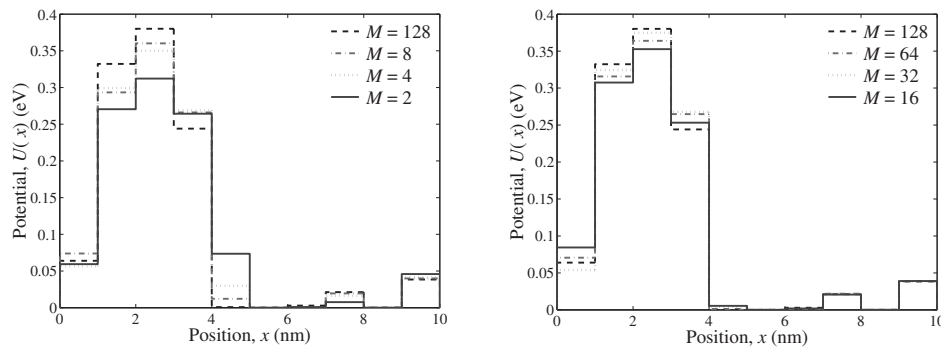


FIG. 5.5. Optimal potential energy profiles for Device 3 given by (5.3) for discretization levels $M = 2, 4, 8, 128$ (left) and $M = 16, 32, 64, 128$ (right).

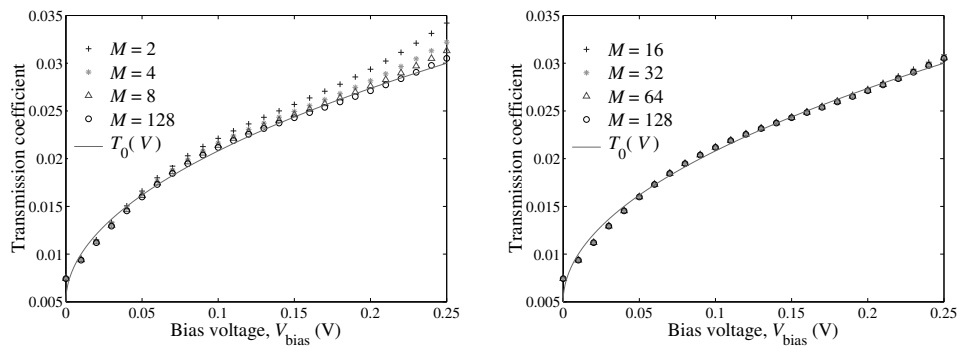


FIG. 5.6. Simulated value of transmission function at bias voltage design values using optimal potential energy profiles for Device 3 given by (5.3) for discretization levels $M = 2, 4, 8, 128$ (left) and $M = 16, 32, 64, 128$ (right).

TABLE 5.4

Tabulated results showing the linear convergence of the gradients of the approximating performance indices predicted in the proofs of Theorems 4.8 and 4.9. The gradients were computed using the adjoint-based scheme discussed in section 3.

| M | 4 | 8 | 16 | 32 | 64 | 128 | 256 | 512 | 1024 |
|--|--------|--------|--------|--------|--------|--------|--------|--------|--------|
| $\ \nabla J^M(\mathbf{U}) - \nabla J^{2048}(\mathbf{U})\ _2$ | 0.0616 | 0.0313 | 0.0157 | 0.0078 | 0.0039 | 0.0019 | 0.0009 | 0.0004 | 0.0001 |
| $\ \nabla J^{2048}(\mathbf{U})\ _2$ | | | | | | | | | |

One might ask how well our approach performs when compared to other schemes for this design problem found in the literature. The only other two treatments with which we are familiar are those detailed in [2] and [3]. In [2] the authors identify the optimal design via an exhaustive search of a discretization of the admissible potential set

$$\Omega = \left\{ \mathbf{U} = \{U_i\}_{i=1}^N \in \mathbf{R}^N : U_L \leq U_i \leq U_H, i = 1, 2, \dots, N \right\}.$$

The level of discretization would depend on the desired degree of precision in the optimal layer potentials. Indeed, if the desired degree of precision in each of the N layer potentials is 10^{-d} , then the number of times that the forward system would

have to be solved in an exhaustive search of the admissible potential set Ω would be approximately $((U_H - U_L) 10^d)^N$. On the other hand, the results presented in Tables 5.1–5.3 required the forward system and the adjoint system to be solved approximately 10 times per iteration. In those examples we had $N = 10$ potential layers, $U_L = 0$ eV, and $U_H = 1$ eV, and the convergence criterion was set at 10^{-12} . So, for example, referring to Table 5.1 with $M = 16$, 41 iterations of the optimization loop were required. Consequently, combining the effort required to solve both the forward and the adjoint system amounted to 2 (forward and adjoint) \times 10 (solutions per iteration) \times 41 (iterations) or 820 system solutions. On the other hand, an exhaustive search of the admissible parameter space to obtain a level of precision of 10^{-12} would have required approximately $((1 - 0) 10^{12})^{10} = 10^{120}$ system solutions.

A meaningful comparison with the approach detailed in [3] is not really possible since the authors in that treatment do not formulate the underlying problem in the same way we did here. Indeed, they take the number of potential layers to be optimized over, N , to be the same as the level of discretization, M . In our case, the number of potential layers is a design criteria set a priori. When M is equal to N , computing the requisite gradients is considerably easier than it is in our setting.

A comparison is possible which highlights the benefits derived from the transformation of the underlying state constraints from a boundary value problem into a terminal value problem and the use of the adjoint method for the efficient computation of gradients. To carry out this comparison we first reformulate the $NM + 1$ 2×2 linear systems in $2NM + 4$ unknowns given in (3.8) and the two boundary conditions given in (3.9) into a single $(2NM + 2)$ -dimensional linear system of equations in $2NM + 2$ unknowns. Indeed, by making use of the boundary conditions (3.9) to move the two determined quantities $A_0^M = A_0$ and $B_{NM+1}^M = 0$ to the right-hand side, we obtain the $(2NM + 2)$ -dimensional linear system

$$(5.4) \quad \mathbf{A}^M(\mathbf{U}, V_{\text{bias}}) \mathbf{X}^M = \mathbf{b}_0^M,$$

where

$$(5.5) \quad \mathbf{X}^M = [B_0^M \quad A_1^M \quad B_1^M \quad A_2^M \quad B_2^M \quad \dots \quad A_{NM}^M \quad B_{NM}^M \quad A_{NM+1}^M]^T,$$

$$\mathbf{b}_0^M = [-A_0 e^{ik_0 x_0} \quad -ik_0 A_0 e^{ik_0 x_0} \quad \mathbf{0} \quad \dots \quad \mathbf{0}]^T,$$

$$\mathbf{A}^M(\mathbf{U}, V_{\text{bias}}) = \begin{bmatrix} \mathbf{v}_0 & \mathbf{Q}_0^M & \mathbf{0} & \dots & \mathbf{0} \\ \mathbf{0} & \mathbf{I} & -\mathbf{P}_1^M & & \vdots \\ & & \mathbf{I} & -\mathbf{P}_2^M & \\ \vdots & & & \ddots & \\ \mathbf{0} & \dots & & \mathbf{I} & -\mathbf{P}_{NM-1}^M & \mathbf{0} \\ & & & \mathbf{0} & \mathbf{Q}_N^M & \mathbf{v}_N \end{bmatrix},$$

with $\mathbf{P}_n^M = \mathbf{P}_n^M(\mathbf{U}, V_{\text{bias}})$, $n = 1, 2, \dots, NM - 1$, are as they were defined in (3.8), \mathbf{I} is the 2×2 identity matrix, $\mathbf{v}_0 = [e^{-ik_0 x_0} \quad -ik_0 e^{-ik_0 x_0}]^T$, $\mathbf{v}_N = [-1 \quad -ik_{N+1}]^T$,

$$\mathbf{Q}_0^M = \begin{bmatrix} -1 & -1 \\ -ik_1^M & ik_1^M \end{bmatrix} \quad \text{and} \quad \mathbf{Q}_N^M = \begin{bmatrix} e^{ik_{NM}^M L_{NM}^M} & e^{-ik_{NM}^M L_{NM}^M} \\ ik_{NM}^M e^{ik_{NM}^M L_{NM}^M} & -ik_{NM}^M e^{-ik_{NM}^M L_{NM}^M} \end{bmatrix}.$$

Under mild assumptions on the total energy E , the layer potentials $\mathbf{U} = \{U_i\}_{i=1}^N$, and the bias voltage V_{bias} , Theorem 4.5 implies that the matrix given in (5.5) is nonsingular and, consequently, that the linear system given in (5.4) admits a unique solution. If, for each $j = 1, 2, \dots, \nu$, we define the $(2NM + 2)$ -dimensional row vector \mathbf{c}_j by

$$\mathbf{c}_j^M = [0 \quad 0 \quad \cdots \quad \sqrt{k_{N+1}} / (\sqrt{k_0} A_0)],$$

the performance index (3.10) can now be written as

$$(5.6) \quad J^M(\mathbf{U}) = \sum_{j=1}^{\nu} \left| T_0(V_j) - \left| \mathbf{c}_j^M \mathbf{X}^M(\mathbf{U}, V_j) \right|^2 \right|^2,$$

where $\mathbf{X}^M(\mathbf{U}, V_{\text{bias}})$ is the unique solution to the linear system (5.4) corresponding to the layer potentials \mathbf{U} and bias voltage V_{bias} .

The gradient with respect to \mathbf{U} , $\nabla J^M(\mathbf{U})$, of the performance index J^M given in (5.6) can also be computed via the application of the static form of the adjoint method described in section 3.2. For each $j = 1, 2, \dots, \nu$, we define the adjoint system by

$$(5.7) \quad \mathbf{A}^M(\mathbf{U}, V_j)^* \mathbf{z}_j^M = 4 (\mathbf{c}_j^M)^* \mathbf{c}_j^M \mathbf{X}_j^M \left(T_0(V_j) - \left| \mathbf{c}_j^M \mathbf{X}_j^M \right|^2 \right),$$

where the entries in the $(2NM + 2)$ -dimensional vector \mathbf{z}_j^M are known as the adjoint or costate variables, $\mathbf{X}_j^M = \mathbf{X}^M(\mathbf{U}, V_j)$ is the unique solution to the linear system (5.4) corresponding to the layer potentials \mathbf{U} and the bias voltage V_j , and \mathbf{A}^* denotes the conjugate transpose of a matrix \mathbf{A} with complex entries. Note that nonsingularity of the matrix $\mathbf{A}^M(\mathbf{U}, V_j)$ given in (5.5) ensures that the adjoint system admits a unique solution \mathbf{z}_j^M . Then

$$(5.8) \quad \begin{aligned} \nabla J^M(\mathbf{U}) &= -2 \sum_{j=1}^{\nu} \left(T_0(V_j) - \left| \mathbf{c}_j^M \mathbf{X}_j^M \right|^2 \right) \left\{ 2 \operatorname{Re} \left(\mathbf{X}_j^M \right)^* (\mathbf{c}_j^M)^* \mathbf{c}_j^M \partial \mathbf{X}_j^M / \partial \mathbf{U} \right\} \\ &= - \sum_{j=1}^{\nu} \operatorname{Re} \left(\mathbf{z}_j^M \right)^* \mathbf{A}^M(\mathbf{U}, V_j) \partial \mathbf{X}_j^M / \partial \mathbf{U} \\ &= \sum_{j=1}^{\nu} \operatorname{Re} \left(\mathbf{z}_j^M \right)^* \left(\partial \mathbf{A}^M(\mathbf{U}, V_j) / \partial \mathbf{U} \right) \mathbf{X}_j^M, \end{aligned}$$

where in the final expression in (5.8) we have used the identity

$$\mathbf{A}^M(\mathbf{U}, V_{\text{bias}}) \left(\partial \mathbf{X}_j^M / \partial \mathbf{U} \right) = - \left(\partial \mathbf{A}^M(\mathbf{U}, V_{\text{bias}}) / \partial \mathbf{U} \right) \mathbf{X}_j^M,$$

which follows immediately by differentiating (5.4). We note that the arguments given in section 4 guarantee that the matrix $\mathbf{A}^M(\mathbf{U}, V_j)$ and the vector $\mathbf{X}_j^M = \mathbf{X}^M(\mathbf{U}, V_j)$ are both differentiable with respect to \mathbf{U} .

It now follows that in each step of an iterative optimization scheme, both the value of the performance index J^M and its gradient $\nabla J^M(\mathbf{U})$ can be computed efficiently by sequentially solving the two linear systems (with only a single LU decomposition

TABLE 5.5

Tabulated results showing CPU time (in seconds) that it took to calculate the value of the performance index J^M and its gradient $\nabla J^M(\mathbf{U})$ for different levels of discretization M for both the boundary value (BV)- and terminal value (TV)-based schemes using both finite differencing (FD) and the adjoint (A) to compute the gradient.

| Method \ M | 2 | 4 | 8 | 16 | 32 |
|--------------|-----|------|-------|-------|--------|
| BV FD | 8.8 | 20.5 | 108.4 | 898.0 | 6611.5 |
| BV A | 1.8 | 4.1 | 21.7 | 179.6 | 1322.3 |
| TV FD | 5.0 | 7.5 | 15.2 | 30.1 | 63.0 |
| TV A | 1.0 | 1.5 | 3.0 | 6.0 | 12.6 |

required because the two system matrices are the same up to conjugate transpose) (5.4) and (5.7),

$$(5.9) \quad \begin{aligned} \mathbf{A}^M(\mathbf{U}, V_j) \mathbf{X}_j^M &= \mathbf{b}_0^M \quad \text{and} \\ \mathbf{A}^M(\mathbf{U}, V_j)^* \mathbf{Z}_j^M &= 4 (\mathbf{c}_j^M)^* \mathbf{c}_j^M \mathbf{X}_j^M \left(T_0(V_j) - \left| \mathbf{c}_j^M \mathbf{X}_j^M \right|^2 \right), \end{aligned}$$

and then computing the sum (5.6) and inner product in the final expression in (5.8) given by

$$(5.10) \quad \begin{aligned} J^M(\mathbf{U}) &= \sum_{j=1}^{\nu} \left| T_0(V_j) - \left| \mathbf{c}_j^M \mathbf{X}_j^M \right|^2 \right|^2, \\ \nabla J^M(\mathbf{U}) &= \sum_{j=1}^{\nu} \text{Re} \left(\mathbf{Z}_j^M \right)^* \left(\partial \mathbf{A}^M(\mathbf{U}, V_j) / \partial \mathbf{U} \right) \mathbf{X}_j^M. \end{aligned}$$

In Table 5.5 we compare the amount of CPU time (in seconds) required to compute the value of the performance index and the gradient for a sample problem involving $N = 10$ potential layers and $\nu = 26$ bias voltages for different levels of discretization M by the boundary value problem formulation just described with the terminal value problem reformulation studied in sections 3 and 4. In each case we compute the gradient using both finite differencing and the adjoint method. It is immediately clear from the table that, for all levels of discretization, in both the boundary value and terminal value formulation, the adjoint method takes about one fifth as much time as the finite-difference method. This is not surprising since with 10 potential layers, the finite-difference method requires 11 system solutions, whereas the adjoint requires only 2 (i.e., the forward system and the adjoint system). What is more striking, however, is the significant savings in time afforded by the use of the terminal value formulation as the level of discretization increases. Indeed, in the case of the terminal value formulation, CPU time grows linearly with M , while in the case of the boundary value formulation, an elementary fit of the data reveals that CPU time growth is proportional to M^α , where α is approximately 2.5.

6. Discussion and conclusion. We have developed a scheme for efficiently identifying optimal designs of electronic devices whose physical behavior is determined by solutions of the Schrödinger equation. Our general approach was illustrated by determining the locally optimal conduction band potential energy profile $V(x)$ for desired electron transmission as a function of applied voltage bias across a semiconductor device. The optimal design problem was formulated as the minimization of a least-squares performance metric. The elastic scattering of an electron incident

on the potential required for the evaluation of the performance metric was calculated by a propagation matrix method that uses a piecewise constant approximation for $V(x)$. The underlying boundary value problem was reformulated as a terminal value problem. In this way the efficient computation of highly accurate gradients of the transmission coefficient with respect to the design parameters in the form of layer potentials required for optimization became amenable to the use of the adjoint method as it is typically applied in the context of evolution equations. We were able to rigorously establish the numerical stability of the method and the convergence of the approximating solutions to the state equations and their gradients with respect to the design parameters as well as the convergence of the solutions to the resulting approximating optimal design problems to an optimal design for the original infinite dimensional device.

Numerical studies show the utility of our approach for achieving control over electron transmission as a function of voltage bias. Linear, square, and square-root dependence of transmission over a finite range of applied bias is achieved, illustrating control over what is typically an exponential dependence of transmission for simpler potential energy profiles. As pointed out in [2], electron transmission is altered by addition of potential energy steps that give rise to broad resonances. Also, as discussed in [2], the superposition of these resonances is both the mechanism by which transmission is controlled and the reason why solutions are stable against small perturbations. The nonmonotone convergence of locally optimal design with increasing discretization observed in Figures 5.1–5.6 may also be attributed to the same superposition of broad resonances due to potential energy steps. The locally optimal potential energy profiles $V(x)$ are nonintuitive in the sense that, at least initially, it is difficult to use previous experience to determine the transmission as a function of potential bias and the range of values of potential bias over which it applies.

Useful extensions of the work presented here include calculation of electron current as a function of applied voltage bias across the device and incorporation of Poisson's equation to solve for finite depletion in the electrodes. Comparing our theoretical predictions with results from laboratory experiments would validate our approach to device design. Also of interest are approaches to global optimization, dimensionality reduction, and robustness that exploit the methods described in this paper.

We anticipate that our general approach could be appropriately modified and be of great help in determining optimal configurations of other forms of electronic devices that operate based on the principles of quantum mechanics. It is a potentially efficient approach to realizing otherwise nonintuitive device designs.

Acknowledgments. The authors would like to gratefully acknowledge the helpful and valuable suggestions of the referees and the Associate Editor.

REFERENCES

- [1] J. THALKEN, Y. CHEN, A. F. J. LEVI, AND S. HAAS, *Adaptive quantum design of atomic clusters*, Phys. Rev. B, 69 (2004), 195410.
- [2] P. SCHMIDT, S. HAAS, AND A. F. J. LEVI, *Synthesis of electron transmission in nanoscale semiconductor devices*, Appl. Phys. Lett., 88 (2006), 013502.
- [3] J. ZHANG AND R. KOSUT, *Robust design of quantum potential profile for electron transmission in semiconductor nanodevices*, in Proceedings of the European Control Conference, Kos, Greece, European Union Control Association, 2007.
- [4] S. WANG, *Fundamentals of Semiconductor Theory and Device Physics*, Prentice-Hall, Englewood Cliffs, NJ, 1989.
- [5] L. I. SCHIFF, *Quantum Mechanics*, McGraw-Hill, New York, 1968.

- [6] A. F. J. LEVI, *Applied Quantum Mechanics*, Cambridge University Press, Cambridge, UK, 2006.
- [7] L. S. PONTRYAGIN, *Optimal regulation processes*, Amer. Math. Soc. Transl., 18 (1961), pp. 321–339.
- [8] L. S. PONTRYAGIN, V. G. BOLTYANSKII, R. V. GAMKRELEDZE, AND E. F. MISCHENKO, *The Mathematical Theory of Optimal Processes*, Interscience, John Wiley & Sons, New York, 1962.
- [9] W. H. FLEMING AND R. W. RISHEL, *Deterministic and Stochastic Optimal Control*, Springer-Verlag, New York, 1975.
- [10] M. D. INTRILLIGATOR, *Mathematical Optimization and Economic Theory*, Prentice-Hall, Englewood Cliffs, NJ, 1971.
- [11] J.-L. LIONS, *Contrôle Optimal de Systèmes Gouvernés par des Équations aux Dérivées Partielles*, Dunod, Gauthier-Villars, Paris, 1968.
- [12] J. MACKI AND A. STRAUSS, *Introduction to Optimal Control Theory*, Springer-Verlag, New York, 1982.
- [13] A. MCNAMARA, A. TREUILLE, Z. POPOVIC, AND J. STAM, *Fluid control using the adjoint method*, in Proceedings of the International Conference on Computer Graphics and Interactive Techniques, ACM SIGGRAPH 2004, Los Angeles, 2004, pp. 449–446.
- [14] R. A. ADAMS, *Sobolev Spaces*, Academic Press, New York, 1975.
- [15] R. E. SHOWALTER, *Hilbert Space Methods for Partial Differential Equations*, Pitman, London, 1977.
- [16] H. TANABE, *Equations of Evolution*, Pitman, Boston, London, 1979.
- [17] J. WLOKA, *Partial Differential Equations*, Cambridge University Press, Cambridge, UK, 1987.
- [18] T. KATO, *Perturbation Theory for Linear Operators*, Springer-Verlag, Berlin, 1976.